The Ross Sea Dipole - Temperature, Snow Accumulation and Sea Ice Variability in the Ross Sea Region, Antarctica, over the Past 2,700 Years

RICE Community

(Nancy A.N. Bertler[1,2], Howard Conway[3], Dorthe Dahl-Jensen[4], Daniel B. Emanuelsson[1,2], Mai Winstrup[4], Paul T. Vallelonga[4], James E. Lee[5], Ed J. Brook[5], Jeffrey P. Severinghaus[6], Taylor J. Fudge[3], Elizabeth D. Keller[2], W. Troy Baisden[2], Richard C.A. Hindmarsh[7], Peter D. Neff[8], Thomas Blunier[4], Ross Edwards[9], Paul A. Mayewski[10], Sepp Kipfstuhl[11], Christo Buizert[5], Silvia Canessa[2], Ruzica Dadic[1], Helle A. Kjær[4], Andrei Kurbatov[10], Dongqi Zhang[12,13], Ed D. Waddington[3], Giovanni Baccolo[14], Thomas Beers[10], Hannah J. Brightley[1,2], Lionel Carter[1], David Clemens-Sewall[15], Viorela G. Ciobanu[4], Barbara Delmonte[14], Lukas Eling[1,2], Aja A. Ellis[16], Shruthi Ganesh[17], Nicholas R. Golledge[1,2], Skylar Haines[10], Michael Handley[10], Robert L. Hawley[15], Chad M. Hogan[18], Katelyn M. Johnson[1,2], Elena Korotkikh[10], Daniel P. Lowry[1], Darcy Mandeno[1], Robert M. McKay[1], James A. Menking[5], Timothy R. Naish[1], Caroline Noerling[11], Agathe Ollive[19], Anaïs Orsi[20], Bernadette C. Proemse[18], Alexander R. Pyne[1], Rebecca L. Pyne[2], James Renwick[1], Reed P. Scherer[21], Stefanie Semper[22], M. Simonsen[4], Sharon B. Sneed[10], Eric J., Steig[3], Andrea Tuohy[23], Abhijith Ulayottil Venugopal[1,2], Fernando Valero-Delgado[11], Janani Venkatesh[17], Feitang Wang[24], Shimeng Wang[13], Dominic A. Winski[15], Victoria H.L. Winton[25], Arran Whiteford[26], Cunde Xiao[27], Jiao Yang[13], Xin Zhang[28])

[1] Antarctic Research Centre, Victoria University of Wellington, Wellington, 6012, New Zealand
[2] GNS Science, Lower Hutt, 5010, New Zealand
[3] Department of Earth and Space Sciences, University of Washington, Seattle, WA 98195, USA
[4] Centre for Ice and Climate, Niels Bohr Institute, University of Copenhagen, Juliane Maries Vej 30, 2100 Copenhagen, Denmark
[5] College of Earth, Ocean, and Atmospheric Sciences, Oregon State University, Corvallis, OR 97330, USA
[6] Scripps Institution of Oceanography, UC San Diego, La Jolla CA 92093, USA
[7] British Antarctic Survey, High Cross, Madingley Road, Cambridge, CB3 0ET, United Kingdom
[8] Antarctic Research Centre, Victoria University of Wellington, Wellington, 6012, New Zealand; Now at University of Rochester, Department of Earth & Environmental Sciences, Rochester, NY, USA 14627
[9] Physics and Astronomy, Curtin University, Perth, Western Australia, Australia
[10] Climate Change Institute, University of Maine, Orono, ME 04469-5790, USA
[11] Alfred Wegner Institute, Bremen, Germany
[12] Chinese Academy of Meteorological Sciences, Beijing, China
[13] State Key Laboratory of Cryospheric Science, Northwest Institute of Eco-Environment and Resources, Chinese Academy of Sciences, Lanzhou, Gansu, China
[14] DISAT, Department of Earth and Environmental Sciences, University Milano-Bicocca, Piazza della Scienza 1, 20126 Milano (Italy)
[15] Department of Earth Sciences, Dartmouth College, 6105 Fairchild Hall, Hanover, NH 03755, USA
[16] Physics and Astronomy, Curtin University, Perth, Western Australia, Australia; Now at Center for Atmospheric Particle Studies, Carnegie Mellon University, Pittsburgh, PA 15213 USA.
[17] Department of Chemical Engineering, SRM University, Kattankulathur - 603203, Kancheepuram Dt., Tamil Nadu, India
[18] University of Tasmania, School of Biological Sciences, Hobart, TAS, 7001 Australia
[19] Specialty of Earth Sciences and Environment, UniLasalle, 19 rue Pierre Waguet, 60000 Beauvais, France

[20] Laboratoire des Sciences du Climat et de l'Environnement, LSCE/IPSL, CEA-CNRS-UVSQ, Université Paris-Saclay, F-91198 Gif-sur-Yvette, France

[21] Northern Illinois University, USA

[22] Geophysical Institute, University of Bergen, and Bjerknes Centre for Climate Research, 5020 Bergen, Norway

[23] Antarctic Research Centre, Victoria University of Wellington and GNS Science, Wellington, New Zealand, now: Tonkin and Taylor, ABS Tower, 2 Hunter St., Wellington, 6011, New Zealand

[24] State Key Laboratory of Cryospheric Science / Tianshan Glaciology Station, Northwest Institute of Eco-Environment and Resources, Chinese Academy of Sciences, Lanzhou, Gansu, China

[25] Physics and Astronomy, Curtin University, Perth, Western Australia, Australia; now at: British Antarctic Survey, Cambridge CB3 0ET, United Kingdom

[26] Department of Earth and Ocean Sciences, University of British Columbia, Canada

[27] State Key Laboratory of Earth Surface Processes and Resource Ecology, Beijing Normal University, Beijing, China

[28] Northwest Normal University, Lanzhou, Gansu, China

Correspondence to: Nancy A.N. Bertler (Nancy.Bertler@vuw.ac.nz)

Abstract. High-resolution, well-dated climate archives provide an opportunity to investigate the dynamic interactions of climate patterns relevant for future projections. Here, we present data from a new, annually-dated ice core record from the eastern Ross Sea. Comparison of the Roosevelt Island Climate Evolution (RICE) ice core records with climate reanalysis data for the 1979-2012 calibration period shows that RICE records reliably capture temperature and snow precipitation variability of the region. RICE is compared with data from West Antarctica (West Antarctic Ice Sheet Divide Ice Core) and the western (Talos Dome) and eastern (Siple Dome) Ross Sea. For most of the past 2,700 years, the eastern Ross Sea was warming with increased snow accumulation and perhaps decreased sea ice extent. However, West Antarctica cooled whereas the western Ross Sea showed no significant temperature trend. From the 17th Century onwards, this relationship changes. All three regions now show signs of warming, with snow accumulation declining in West Antarctica and the eastern Ross Sea, but increasing in the western Ross Sea. Analysis of decadal to centennial-scale climate variability superimposed on the longer term trend reveal that periods characterised by opposing temperature trends between the Eastern and Western Ross Sea have occurred since the 3rd Century but are masked by longer-term trends. This pattern here is referred to as the Ross Sea Dipole, caused by a sensitive response of the region to dynamic interactions of the Southern Annual Mode and tropical forcings.

1 Introduction

With carbon dioxide (CO_2) and global temperatures predicted to continue to rise, model simulations of the Antarctic / Southern Ocean region show for the coming decades an increase in surface warming resulting in reduced sea ice extent, weakened Antarctic Bottom Water formation, intensified zonal winds that reduce CO_2 uptake by the Southern Ocean, a slowing of the southern limb of the meridional overturning circulation (MOC) and associated changes in global heat transport, and rapid ice sheet grounding line retreat that contributes to global sea level rise (Russell et al., 2006; Toggweiler and Russell, 2008; Anderson et al., 2009; Sen Gupta et al., 2009; Downes et al., 2010; Joughin and Alley, 2011; Marshall and Speer, 2012; Spence et al., 2012; Kusahara and Hasumi, 2013; Golledge et al., 2015; DeConto and Pollard, 2016; DeVries et al., 2017). Observations confirm an ozone-depletion-induced strengthening and poleward contraction of zonal winds (Thompson and Solomon, 2002b; Arblaster et al., 2011), increased upwelling of warm, modified Circumpolar Deep Water (Jacobs et al., 2011), a warmer Southern Ocean (Gille, 2002; Böning et al., 2008; Abraham et al., 2013), meltwater-driven freshening of the Ross Sea (Jacobs et al., 2002), ice shelf and mass balance

loss, grounding line retreat (Joughin et al., 2014; Rignot et al., 2014; Paolo et al., 2015; Pollard et al., 2015), reduced formation of Antarctic Bottom Water (Rintoul, 2007) and Antarctic Intermediate Water (Wong et al., 1999), changes in sea ice (wind driven, regional increase and decrease in the Amundsen and Ross Seas, respectively) (Holland and Kwok, 2012; Stammerjohn et al., 2012; Sinclair et al., 2014), and dynamic changes of Southern Ocean CO_2 uptake driven by atmospheric circulation pattern

5   (Landschützer et al., 2015). Yet, these observational time series are short (Gille, 2002; Böning et al., 2008; Toggweiler and Russell, 2008) and inter-model variability indicates physical processes and their consequences are not well captured or understood (Sen Gupta et al., 2009; Braconnot et al., 2012). While the skill of equilibrium simulations steadily improves, the accuracy of transient model projections for the coming decades critically depends on an improved knowledge of climate variability, forcings, and dynamic feedbacks (Bakker et al., 2017; Stouffer et al., 2017).

10 Here we present data from a new, highly-resolved and accurately-dated ice-core record, spanning the past 2.7 ka, from the Ross Sea region. The Roosevelt Island Climate Evolution (RICE) ice core is compared with existing records in the region to investigate the characteristics and drivers of spatial and temporal climate variability in the Ross Sea region.

2   Site characteristics and relevant climate drivers

15 In this section, a brief overview is provided of the climatological and glaciological characteristics of the study site.

2.1   Dynamic interaction between tropical and mid-latitudinal climate drivers and South Pacific climate variability

Environmental conditions in the Pacific Sector of the Southern Ocean and Antarctica are dominated by four major atmospheric circulation patterns: the Southern Annular Mode (SAM), the Pacific-South American pattern (PSA1 and PSA2) that are related to El Niño Southern Oscillation (ENSO) variability, and the Inter-decadal Pacific Oscillation (IPO). The SAM, the leading

20 empirical orthogonal function (EOF) of the Southern Hemisphere extratropical geopotential height fields on monthly and longer time scales, describes the strength and position of the Southern Hemisphere westerly winds via the relative pressure anomalies over Antarctica (~65°S) and the mid-latitudes (~45°S) (Thompson and Wallace, 2000; Thompson and Solomon, 2002a). The persistent positive, summer trend of the SAM (decreasing pressure over Antarctica) has been linked to stratospheric ozone depletion and increase in atmospheric greenhouse gas concentration (Arblaster et al., 2011; Thompson et

25 al., 2011). The positive SAM is associated with above average warming of the Antarctic Peninsula, and cooler conditions over East Antarctica due to a reduced poleward gradient and thus diminished transport of heat and moisture along with a reduction in katabatic flow (Thompson and Solomon, 2002a; Marshall et al., 2013; Marshall and Thompson, 2016). While the positive summer SAM trend (also weakly expressed during autumn) along the Antarctic margin is generally associated with an equatorward heat flux, the western Ross Sea is one of two regions (the Weddell Sea being the other) to experience an anomalous

30 poleward heat flux (Marshall and Thompson, 2016), that transports heat and moisture across the Ross Ice Shelf. The positive SAM has been shown to contribute at least partially to an Antarctic SIE increase, while a negative SAM has been associated with a reduced SIE (Bintanja et al., 2013; Ferreira et al., 2015; Kohyama and Hartmann, 2015; Holland et al., 2016; Turner et al., 2017). The future behaviour of the SAM over the next decades is a topic of active research due to the competing, and seasonally biased influences of projected stratospheric ozone recovery and greenhouse gas emissions (Thompson et al., 2011;

35 Gillett and Fyfe, 2013; Bracegirdle et al., 2014).

PSA patterns represent atmospheric Rossby wave trains initiated by anomalously deep tropical convection during ENSO events, in particular during austral spring, which originate in the western (PSA1) and the central (PSA2) tropical Pacific (Mo and Higgins, 1998). PSA1 and PSA2 are defined as the 2nd and 3rd EOF respectively of monthly-mean extratropical geopotential height fields, with the negative (positive) phase resembling El Niño (La Niña)-like conditions (Mo, 2000).

40 Changes in SAT over West Antarctica have been linked to PSA1 variability (Schneider and Steig, 2008; Schneider et al.,

2012), while the warming of West Antarctica's winter temperatures has been linked to PSA2 (Ding et al., 2011). The positive polarity of PSA1 is associated with anticyclonic wind anomalies in the South Pacific centered at ~120°W, which have been linked to increased onshore flow and increased eddy activity (Marshall and Thompson, 2016; Emanuelsson et al., in review). In contrast, during the positive phase of the PSA2, the anticyclonic centre shifts to ~150°W in the Ross Sea, creating a dipole

5   across the Ross Ice Shelf, with increased transport of marine air masses along the western Ross Ice Shelf and enhanced katabatic flow along the eastern Ross Ice Shelf (Marshall and Thompson, 2016). Sea ice feedbacks to the SAM and ENSO forcing in the western Ross Sea (as well as the Bellingshausen Sea) were found to be particularly strong when a negative SAM coincided with El Niño events (increased poleward heat flux, less sea ice) or a positive SAM concurred with La Niña events (decreased poleward heat flux, more sea ice) (Stammerjohn et al., 2008). The authors found that this teleconnection is less

10   pronounced in the eastern Ross Sea.

The Inter-decadal Pacific Oscillation (IPO), an ENSO-like climate variation on decadal time scales (Power et al., 1999), is closely related to the Pacific Decadal Oscillation (PDO) (Mantua and Hare, 2002). While the PDO is defined as the first EOF of sea surface temperature (SST) variability in the Northern Pacific, the IPO is defined by a tripole index of decadal scale SST anomalies across the Pacific (Henley et al., 2015). A warm tropical Pacific and weakened trade winds are associated with a

15   positive IPO, while a cooler tropical Pacific and strengthened trade winds are characteristic for a negative IPO. The phasing of the IPO and PDO have been shown to influence the strength of regional and global teleconnections with ENSO (Henley et al., 2015). An in-phase IPO amplification of ENSO events has been linked to a strengthening of global dry / wet anomalies, in contrast to periods when the IPO and ENSO are out of phase, causing these anomalies to weaken or disappear entirely (Wang et al., 2014). In addition, a negative IPO leads to cooler SSTs in the Ross, Amundsen and Bellingshausen Seas, while a positive

20   IPO is associated with warmer SSTs (Henley et al., 2015). The centre of anticyclonic circulation linked to precipitation at Roosevelt Island (Emanuelsson et al., in review) moves eastward during the negative IPO from ~120°W during the positive IPO to ~100°W (Henley et al., 2015). It has been suggested that the negative IPO, at least in part, is responsible for the hiatus of global surface warming during 1940-1975 and 2001-2009 (Meehl et al., 2011; Kosaka and Xie, 2013; England et al., 2014).

The Amundsen Sea Low (ASL), a semi-permanent low pressure centre in the Ross / Amundsen Sea, is the most prominent

25   and persistent of three low pressure centres around Antarctica, associated with the wave number 3 circulation (Raphael, 2004). The ASL is sensitive to ENSO (especially during winter and spring) and SAM (in particular during autumn) and to influence through meridional wind anomalies environmental conditions in the Ross, Amundsen and Bellingshausen Seas and across West Antarctica and the Antarctic Peninsula (Bertler et al., 2004; Thomas et al., 2009; Steig et al., 2012; Ding and Steig, 2013; Turner et al., 2013; Marshall and Thompson, 2016; Raphael et al., 2016). Seasonally, the ASL centre moves from ~110°W in

30   during austral summer to ~150°W austral winter (Turner et al., 2013). A positive SAM and / or La Niña event leads to a deepening of the ASL, while a negative SAM and/or El Niño event causes a weakening (Turner et al., 2013). The IPO, through its effect upon ENSO and SAM variability, also influences the ASL and sea ice extent in the Ross and Amundsen seas (Meehl et al., 2016). Blocking events in the Amundsen Sea (Renwick, 2005), are sensitive to the position of the ASL and are dominant drivers of marine air mass intrusions and associated precipitation and temperature anomalies at Roosevelt Island (Emanuelsson

35   et al., in review).

2.2   RICE site characteristics

Roosevelt Island is an approximately 120 km-long by 60 km-wide grounded ice rise located near the north-eastern edge of the Ross Ice Shelf (Figure 1). Ice accumulates locally on the ice rise, while the floating Ross Ice Shelf flows around Roosevelt

40   Island. The ice surrounding Roosevelt Island originates from the West Antarctic Ice Sheet (WAIS), via the Bindschadler, MacAyeal and Echelmeyer ice streams. Bedmap2 data (Fretwell et al., 2013) suggest that the marine basins on either side of Roosevelt Island are roughly 600 m (western basin) and 750 m (eastern basin) deep and that the thickness of the Ross Ice Shelf

at this location is about 500 m. At the RICE drill site (79.39S, 161.46W, 550 m above sea level) near the summit of Roosevelt Island, the ice is 764 m thick and grounded 214 m below sea level. Radar surveys across the Roosevelt Island ice divide show a well-developed "Raymond Bump" (Raymond, 1984) arching of isochrones suggesting a stable ice divide (Conway et al., 1999). The vertical velocity, constrained by phase-sensitive radio echo sounder (pRES) measurements, is approximately 20

5 cm a^{-1} at the surface relative to the velocity of 0 cm a^{-1} at the bed (Kingslake et al., 2014).

3 Ice core data

During two field seasons, 2011-2012 and 2012-2013, a 764 m-long ice core to bedrock was extracted from the summit of Roosevelt Island. The drilling was conducted using the New Zealand intermediate depth ice core drill *Te Wāmua Hukapapa*

10 ('Ice Cores That Discover the Past' in NZ Te Reo native language). The drill system is based on the Danish Hans Tausen Drill with some design modification (Mandeno et al., 2013). The upper 60 m of the borehole was cased with plastic pipe and the remainder of the drill hole filled with a mixture of Estisol-240 and Coasol to prevent closure. The part of the RICE ice core record used in this study covers the past 2.7 ka and consists of data combined from the RICE-2012/13-B firn core (0.56-12.30 m depth) and the RICE Deep ice core (12.30 m – 344 m depth). An overview of the core quality and processing procedures

15 are summarised by Pyne et al. (in review). In this manuscript, we present new water stable-isotope (deuterium, δD) and snow accumulation records and compare them with existing records from West and East Antarctica (Table 1).

3.1 RICE age model: RICE17

The RICE17 age model for the past 2.7 ka is based on an annually-dated ice core chronology from 0-344 m which is described

20 in detail by Winstrup et al. (in preparation). The cumulated age uncertainty for the past 100 years is ≤ ±2 years, for the past 1,000 years ≤ ±19 years and for the past 2,000 years ≤ ±38 years, reaching a maximum uncertainty of ±45 years at 344 m depth (2.7 ka). The RICE17 timescale is in good agreement with the WD2014 annual-layer counted timescale from the WAIS Divide ice core dating to 200 Common Era (CE, 280 m depth). For the deeper parts of the core, there is likely a small bias (2-3%) towards undercounting the annual layers, resulting in a small age offset compared to the WD2014 timescale (Winstrup et

25 al., in preparation).

3.2 Snow accumulation reconstruction

Ice core annual layer thicknesses provide a record of past snow accumulation once the amount of vertical strain has been accounted for. At Roosevelt Island, repeat pRES measurements were performed across the divide, providing a direct

30 measurement of the vertical velocity profile (Kingslake et al., 2014). This has a key advantage over most previous ice-core inferences of accumulation rate because vertical strain thinning through the ice sheet is measured directly, rather than needing to use an approximation for ice-flow near ice divides (e.g. Dansgaard and Johnsen, 1969; Lliboutry, 1979). Uncertainty in the accumulation-rate reconstruction increases from zero at the surface (no strain thinning) to a maximum of ± 8 % at 170 m true depth. Below 170 m, the uncertainty remains constant at ± 8 %. A detailed description of the accumulation-rate reconstruction

35 is provided by Winstrup et al. (in preparation).

3.3 Water stable-isotope data

The water stable-isotope record was measured using a continuous-flow laser spectroscopy system with an off-axis integrated cavity output spectroscopy (OA-ICOS) analyser, manufactured by Los Gatos Research (LGR). The water for these

measurements was derived from the inner section of the continuous flow analysis (CFA) melt head, while water from the outside section was collected for discrete samples. A detailed description and quality assessment of this system is provided by Emanuelsson et al. (2015). The combined uncertainty for deuterium (δD) at 2 cm resolution is ±0.85‰. A detailed description of the isotope calibration, the calculation of cumulative uncertainties, and the assignment of depth is provided by Keller et al.

5   (in preparation).

4   RICE data correlation with reanalysis data - modern temperature, snow accumulation, and sea ice extent trends

The ERA-Interim (ERAi) reanalysis data set of the European Centre for Medium-Range Weather Forecasts (ECMWF, Dee et al., 2011), along with firn and ice cores, snow stakes and an automatic weather station (AWS) are used to characterise the

10   meteorological characteristics of Roosevelt Island. ERAi data have been extracted for the RICE drill site from the nearest grid point (S 79.50°, W 162.00°, Figure 1b) for the common time period between 1979 and 2012. The year 1979, the onset of the ERAi reanalysis, occurs at 13.42 m depth in the firn. For this reason, the period 1979-2012 is predominantly captured in the RICE 12/13 firn core. Data from the RICE AWS suggest that precipitation at RICE can be irregular, with large snow precipitation events dominating the accumulation pattern (Emanuelsson, 2016). Therefore, we limit the analysis in this study

15   to annual averages and longer-term trends.

4.1   Isotope-temperature correlation

In Figure 2a, the ERAi surface air temperature (SAT) time series extracted for the RICE drill site is compared with the ERAi SAT spatial grid. The analysis suggests that temperature variability at RICE is representative of variability across the Ross Ice

20   Shelf (with the exception of the western-most margin along the Transantarctic Mountains), Northern Victoria Land, western Marie Byrd Land, and the Ross and Amundsen Seas. Furthermore, the Antarctic Dipole pattern (Yuan and Martinson, 2001), a negative correlation between the SAT in the Ross / Amundsen Sea region and that of the Weddell Sea, is also captured in the data. The locations of the Siple Dome, WDC and TALDICE ice cores all within the region of positive RICE SAT correlation.

25   However, the correlation between RICE δD data and ERAi SAT is limited (Figure 2b), retaining a positive correlation across the Ross Ice Shelf and northern Ross Sea. The time series correlation between the ERAi SAT record and the RICE δD data (Figure 2d) is r=0.45 (p<0.01). We test the robustness of this relationship by applying the minimum and maximum age solutions within the age uncertainty (≤ 2 year during this time period, Winstrup et al., in preparation) to identify the age model solution within the age uncertainty that renders the highest correlation. This optimised solution RICE δD_o is shown in Figure

30   2e with a correlation coefficient of r=0.75 (p<0.001). The correlation of the RICE δD_o record with the ERAi SAT data (Figure 2b) produces a pattern that closely resembles the correlation pattern using the ERAi data itself (Figure 2a), suggesting that the δD record provides useful information about the regional temperature history.

From the comparison between RICE δD_o and ERAi SAT records, we obtain a temporal slope of 5.50 ‰ °C^{-1} (Figure 2f), which falls within the lower limit of previously reported values from Antarctica of ~5.56 ± 0.51 ‰ °C^{-1} to ~6.80 ± 0.57 ‰ °C^{-1}

35   (Schneider et al., 2005; Masson-Delmotte et al., 2008; Fegyveresi et al., 2011). We use this relationship to calculate temperature variations for the RICE δD record. The average annual temperature calculated for 1979-2012 from ERAi for the RICE site is -27.4 ± 2.4 °C and for the δD_o data: -27.5 ± 3.1 °C. Although the year to year SAT variability appears to be well captured in the RICE δD_o record, there are discrepancies in observed trends. While RICE δD_o data suggest an increase in SAT from 1996 onwards, ERAi SAT data do not show a trend (Figure 2e). It remains a challenge to determine how well reanalysis

40   products, including ERAi data, and other observations capture temperature trends in Antarctica (Pages 2k Consortium, 2013;

Stenni et al., 2017) and thus whether the observed difference in trend between ice core δD_o and ERAi SAT is significant or meaningful.

Furthermore, we test the correlation with the near surface Antarctic temperature reconstruction (NB2014, Nicolas and Bromwich, 2014) , which uses three reanalysis products and takes advantage of the revised Byrd Station temperature record

5 (Bromwich et al., 2013) to provide an improved reanalysis product for Antarctica for the time period 1958-2012 CE. We find no correlation between the NB2014 records and the ERAi data at the RICE site, nor the RICE δD data for the 1979-2012 time period, perhaps suggesting some regional challenges.

4.2 Regional snow accumulation variability

10 Temporal and spatial variability of snow accumulation are assessed using 144 snow stakes covering a 200 km² array. The 3 m long, stainless steel poles were set and surveyed in November 2010, re-measured in January 2011, and revisited and extended in January 2012 and November 2013. The measurements indicate a strong accumulation gradient with up to 32 cm water equivalent per year (weq a-1) on the north-eastern flank decreasing to 9 cm weq a-1 on the south-western flank. Near the drill site, annual average snow accumulation rates range from 20-30 cm weq a^{-1} from 2010 to 2013. Investigation of snow

15 precipitation events as captured by ERAi data shows that large snow precipitation events are associated with north-easterly flow (Emanuelsson et al., in review).

Additionally, the RICE AWS included a Judd Ultrasonic Depth Sensor for snow accumulation measurements. The sensor was positioned 140-160 cm above the ground and reset during each season. The 3-year record shows gaps (Figure 3) which represent times when rime precipitation on the sensor caused snow height to be erroneously recorded at the same height as the

20 sensor. This process was particularly prevalent during winter. Over the three years, the site received an average annual snow pack of ~75 cm. These data represent height measurements and are not corrected for snow density. The ERAi data have been shown to best capture snow precipitation variability in Antarctica, but to perhaps underestimate the total amount (Sinclair et al., 2010; Bromwich et al., 2011; Wang et al., 2016). The ERAi data are not directly comparable to the AWS data presented here, as the ERAi data are reported in cm weq and do not capture periods of snow removal through wind scouring. Yet, there

25 is a good agreement between the two data sets with respect to the relative rate of precipitation, which suggests neither winters nor summers have been times of significant snow removal. However, the ERAi data suggest an average annual snow accumulation of only 11 cm weq a^{-1}. The average annual snow accumulation rate derived from the RICE ice core (Winstrup et al., in preparation) is 21 ± 0.06 cm weq a^{-1} for the same time period (1979-2012). Assuming an average density of 0.37 g/cm³ (average density in two snow pits, 0-75 cm), the AWS data suggest 20 cm weq a^{-1} snow accumulation, which is

30 comparable to our ice core snow accumulation rate. We attribute this difference to the spatial differences between measurements of the snow stake array, the interpolation field of the nearest ERAi data point, and the actual drill site location. The regional representativeness of RICE snow accumulation data is assessed by correlating the ERAi precipitation time series, extracted for the RICE location, with the ERAi precipitation grid data (Figure 4a). The correlation suggests that precipitation variability at Roosevelt Island is representative of the observed variability across the Ross Ice Shelf, the southern Ross Sea,

35 and western West Antarctica. We note from Figure 4a that the sites of the Siple Dome ice core (green circle) and the West Antarctic Ice Sheet Divide ice core (WDC, red circle) are situated within the positive correlation field, while Talos Dome (TALDICE, purple circle) shows no correlation to ERAi precipitation at RICE. A negative correlation is found with the region of the Amundsen Sea Low (ASL) (Turner et al., 2013; Raphael et al., 2016). In Figure 4b, the RICE snow accumulation record is correlated with ERAi precipitation data and shows similar pattern. The resemblance of the correlation patterns suggests that

40 the variability of the RICE snow accumulation data (Figure 4b) reflects regional precipitation variability (Figure 4a) and thus likely can elucidate regional snow accumulation variability in the past, in particular for array reconstructions such as i.e. Thomas et al. (2017). We also test the correlation with the optimised age scale derived for the δD_o record and find that for

snow accumulation data this adjusted age scale (Acc$_o$) reduces the correlation but remains statistically significant (Table 2). We note that the sensitivity of the correlation to those minor adjustments is founded in the brevity of the common time period. However, none of the overall pattern and relationships changes significantly between the two age scale solutions.

4.3 Influence of regional sea ice variability on RICE isotope and snow accumulation

Sea ice extent (SIE) variability has been shown to influence isotope values in precipitated snow, particularly in coastal locations (Noone and Simmonds, 2004; Thomas and Bracegirdle, 2009; Küttel et al., 2012) through the increased contribution of enriched water vapour during times of reduced sea ice and increased sensible heat flux due to a higher degree of atmospheric stratification leading to more vigorous moisture transport. Tuohy et al. (2015) demonstrated that for the period 2006-2012 ~40-60% of precipitation arriving at Roosevelt Island came from local sources in the southern Ross Sea. In addition, Emanuelsson et al. (in review) demonstrated the important role of blocking events, that are associated with over 88% of large precipitation events at RICE, on sea ice variability via meridional wind field anomalies.

Snow accumulation at RICE is negatively correlated with SIE in the Ross Sea region (Figure 5a), with years of increased (decreased) SIE leading to reduced (increased) accumulation at RICE, confirming the sensitivity of moisture-bearing marine air mass intrusions to local ocean moisture sources and hence regional SIE. The correlation between ERAi SIE and the optimised RICE δD_o record (Figure 5b) similarly shows a negative correlation of SIE in the Ross Sea (perhaps with the exception of the Ross and Terra Nova polynyas) suggesting more depleted (enriched) values during years of increased (reduced) SIE.

To investigate the relationship between the Ross Sea SIE and the temperature and precipitation at Roosevelt Island, the Ross-Amundsen Sea SIE index (SIE$_J$) developed by Jones et al. (2016) is correlated with ERAi SAT and precipitation data (Figure 5 c and d). We focus on the SIE in the Ross and Amundsen Seas (as defined by Jones et al. 2016). Here, the analysis also identifies the co-variance of SIE and SAT, with increasing (decreasing) sea ice coinciding with cooler (warmer) SAT. This suggests that during years of increased SIE, the Ross Ice Shelf and western Marie Byrd Land experience lower temperatures and less snow accumulation. The correlation between SIE$_J$ and ERAi precipitation at RICE is r= –0.67, and for SIE$_J$ and RICE snow accumulation r= –0.56 (Table 2). Moreover, the correlation between SIE$_J$ and ERAi SAT and SIE$_J$ and RICE δD_o is also statistically significant with r= –0.38 and r= –0.53, respectively. The higher correlation with RICE δD_o perhaps suggests that the influence of SIE in the Ross Sea region affects the RICE δD record both through direct temperature changes in the region as well as fractionation processes that are independent of temperature, such as the lengthened distillation pathway to RICE during periods of more extensive SIE.

The ERAi SAT and ERAi precipitation data at RICE (Table 2) reveal a positive correlation over large areas of Antarctica with higher correlation coefficients over the eastern Ross Sea and eastern Weddell Sea (spatial fields not shown). At the RICE site, the correlation reaches r=0.66 (p<0.001). Moreover, the correlation between RICE δD and RICE Acc [or RICE δD_o and RICE Acc$_o$] data yield a statistically significant correlation of r=0.40 (p<0.05) [or r$_o$=0.45, p$_o$<0.01], respectively. This suggests that years with positive isotope anomalies are frequently characterised by higher snow accumulation rates. In contrast, precipitation during low snow accumulation years might be dominated by precipitation from air masses that have travelled further and perhaps across West Antarctica (Emanuelsson et al., in review) leading to more depleted isotope values and lower snow accumulation rates than local air masses from the Ross Sea region.

4.4 Influence of climate drivers on prevailing conditions in the Ross Sea region

Seasonal biases and the enhancing or compensating effects of the relative phasing of SAM, ENSO, and IPO conditions, on seasonal, annual and decadal time scales, make linear associations of climate conditions and their relationship with climate

drivers in the South Pacific challenging. We use the SAM$_A$ index developed by Abram and colleagues (2014) to test the fidelity of the SAM relationship with the climatic conditions in the Ross Sea over the past millennium (Table 2). In addition, the Southern Oscillation Index (SOI, Trenberth and Stepaniak, 2001) and Niño 3.4 index (Rayner et al., 2003) for PSA1, the Niño 4 Index (Trenberth and Stepaniak, 2001) for PSA2, along with the IPO Index (Henley et al., 2015) are used to investigate the

5 influence of SST variability in the eastern (PSA1) and central (PSA2) tropical Pacific on annual and decadal time scales (IPO). In addition, we take advantage of a 850-year reconstruction of the Niño 3.4 index (Emile-Geay et al., 2013) to investigate any long term influence of the eastern Pacific SST on environmental conditions in the Ross Sea.

The correlation of ERAi data and modern ice core records covering the 1979-2012 CE period with indices of relevant climate drivers (Table 2) suggests that SAM$_A$ has an enduring statistically significant relationship with temperature, snow

10 accumulation and SIE in the Ross Sea, with the positive SAM being associated with cooler temperatures, lower snow accumulation / precipitation and more extensive SIE. The correlations remain robust and at comparable levels using a detrended SAM$_A$ record. In contrast, ENSO (SOI, Niño 3.4 and 4) and ENSO-like variability (IPO) have only linear statistically significant relationships with ERAi precipitation (but not with RICE snow accumulation) and SIE$_J$. The dynamic relationship between the phasing of SAM, PSA 1 and 2, and IPO maybe masking aspects of the interactions (Fogt and Bromwich, 2006;

15 Emanuelsson, 2016; Marshall and Thompson, 2016). We note that the influence of SAM and PSA2 lead to a climate dipole within the Ross Ice Shelf / Ross Sea Region with opposing trends of meridional heat flux and near surface winds between the eastern and western Ross Ice Shelf / Ross Sea region. In contrast, the teleconnections with the PSA1 and IPO cause changes that affect uniformly the entire Ross Ice Shelf / Ross Sea Region but with opposing effects in West Antarctica (Marshall and Thompson, 2016).

5   Temperature and snow accumulation variability over the past 2.7 ka

Decadally-smoothed RICE isotope and snow accumulation records for the past 2.7 ka (Figure 6) are compared with published data from the Ross Sea region (Siple Dome – green), coastal East Antarctica (Talos Dome / TALDICE – purple) and West Antarctica (West Antarctic Ice Sheet Divide Ice Core / WDC - red).

25 ### 5.1   Temperature Variability

We find that the RICE and Siple Dome (Brook et al., 2005; WAIS Divide Project Members, 2013) isotope records share a long-term warming trend in the Ross Sea Region. In contrast, WDC isotope (Steig et al., 2013) and borehole temperature data (Orsi et al., 2012) exhibit a long-term cooling trend for West Antarctica, while TALDICE recorded stable conditions for coastal East Antarctica in the western Ross Sea.

30 Elevation changes influence water isotope values (Vinther et al., 2009). Thinning of Roosevelt Island, inferred from the amplitude of arched isochrones beneath the crest of the divide and the depth-age relationship from the ice core (Conway et al., 1999, H. Conway, personal communication) is less than 2 cm a^{-1} for the past 3.5 ka. That is, the surface elevation has decreased less than 50 m over the past 2.7 ka. Assuming that these elevation changes are sufficient to influence vertical movement of the precipitating air mass, such an elevation change could account for an isotopic enrichment of ~2 ‰ (Vinther et al., 2009), which

35 is insufficient to explain the total observed increase of 8 ‰. Furthermore, the RICE δD trend is characterised by two step-changes at 579 CE ± 27 years and 1492 CE ± 10 years (grey dotted lines in Figure 6), when decadal isotope values increase by 3 ‰ and 5 ‰, respectively, which suggests that elevation changes were not a principal driver. Using the temporal slope of 5.5‰ per °C, these abrupt temperature transitions represent an increase of the average decadal temperature (Figure 7a) from -29.5 °C to -29.0 °C and from -29.0 °C to -28.0 °C, respectively. An underlying influence from long-term thinning, accounting

40 for a δD shift of 2.4‰, would exaggerate the observed warming of 1.5 °C by 0.4 °C, thus suggesting a minimum warming of

at least 1.1 °C. The modern decadal isotope temperature average (2003-2012) of –26.3 °C (pink bar, Figure 7a) and ERAi temperature of -26.5 °C lie within the 2 σ distribution of the natural decadal temperature variability of the past 500 years.

The Siple Dome ice core δ¹⁸O record exhibits a similar isotope history to the RICE δD record. Siple Dome isotope data reveal an abrupt warming at 605 CE, some 27 years later than in RICE, but within the cumulative age uncertainty of the two records.

5 After 605 CE, Siple Dome temperatures remain stable, although recording somewhat warmer temperatures from about 1875 CE. Late-Holocene elevation changes (thinning) at Siple Dome have been reported to be negligible (Price et al., 2007) and are unlikely to have caused the observed abrupt warming at 605 CE. In contrast to records from the western Ross Sea (Stenni et al., 2002; Bertler et al., 2011; Rhodes et al., 2012) and West Antarctica (Orsi et al., 2012), RICE and Siple Dome do not show a warming or cooling associated with the Medieval Warm Period (MWP) or the Little Ice Age (LIA), respectively.

10 The WDC δ¹⁸O record suggests a long-term isotope cooling of West Antarctica, confirmed by borehole temperature reconstructions (Orsi et al., 2012). This trend is consistent with warmer-than-average temperatures during the MWP and cooler conditions during the LIA, but may also reflect changes in elevation and decreasing insolation (Steig et al., 2013). The cooling trend is followed by an increase in temperature in recent decades (Steig et al., 2009; Orsi et al., 2012) consistent with an increase in marine air mass intrusions (Steig et al., 2013). We note that 579 CE marks the onset of a decline in WDC isotope

15 and borehole temperatures, in line with the observed anti-phase relationship of WDC with RICE and Siple Dome. No notable change is observed in WDC water stable-isotope temperature data in the late 15ᵗʰ Century. In contrast, WDC borehole temperature suggests the onset of a warming trend within the last 100 years, marking the modern divergence between WDC isotope and borehole records. The TALDICE water stable-isotope temperatures does not exhibit a long term trend over the past 2.7 ka. Yet colder water stable-isotope temperature anomalies have been associated with the LIA period (Stenni et al.,

20 2002), which coincide approximately with the intensified warming at RICE and cooler conditions at WDC.

The similarity between the RICE and Siple Dome records suggests that the eastern Ross Sea was dominated by regionally-coherent climate drivers over the past 2.7 ka, perhaps receiving precipitation via similar air-mass trajectories. Overall this comparison shows that temperature trends in the eastern Ross Sea (warming at RICE and Siple Dome) and West Antarctica (WDC cooling) were anti-phased for over 2 ka (660 BCE to ~1500 CE), while the western Ross Sea (TALDICE) remained

25 stable. From the 17ᵗʰ Century onwards, while WDC water stable isotope temperatures continue to cool, the WDC borehole temperature record a warming, in phase with RICE and Siple Dome and concomitant with warmer temperatures at TALDICE.

5.2 Snow accumulation variability

Investigating long-term trends in snow accumulation records (Figure 6b), the decadally-smoothed RICE (Winstrup et al., in

30 preparation) show a discernible positive trend from about 600 CE. TALDICE data (Stenni et al., 2011) show a long term increase in snow accumulation rates for the eastern and western Ross Sea, respectively, while WDC (Fudge et al., 2016) displays a decreasing trend for central West Antarctica. The RICE snow accumulation data reach a maximum in the 13ᵗʰ Century, with a trend towards lower values from 1686 CE onward. Based on the strong, negative correlation between RICE snow accumulation and SIE in recent decades, we interpret the long-term increase in snow accumulation to represent a long

35 term reduction in SIE the Ross Sea, consistent with a long term increase in RICE isotope temperature. The modern decadal average (2002-2012) of 20 cm weq a⁻¹ lies within the 2 σ variability of decadal RICE ice core snow accumulation rates (Figure 7). TALDICE records its maximum in the 20ᵗʰ Century and had a positive trend perhaps commencing in the 15ᵗʰ Century. Until the 15ᵗʰ Century, snow accumulation and isotope data show an expected positive correlation for all three ice cores RICE, WDC and TALDICE. Regionally, RICE and TALDICE snow accumulation trends are in phase, while being out of phase with WDC.

40 From the 16ᵗʰ Century, this relationship reverses and RICE and WDC snow accumulation are now in phase, suggesting below average snow accumulation in the eastern Ross Sea and West Antarctica. However, TALDICE records above average snow accumulation in the western Ross Sea region. We note that from the 16ᵗʰ Century snow accumulation at RICE and WDC

display a negative correlation with water stable isotope (RICE) and borehole temperature (WDC) reconstructions, respectively. At RICE this relationship is again positive for 1979-2012.

6   Drivers and patterns of decadal to centennial climate variability

Paleo-reconstructions of the SAM$_A$ (Abram et al., 2014) and Niño 3.4 (Emile-Geay et al., 2013) indices (Figure 6) provide important opportunities to investigate the influence of dominant drivers of regional climate conditions over the past millennium. The Niño 3.4 index captures in particular the ENSO signal originating in the central-eastern tropical Pacific associated with the PSA1 pattern. Emile-Geay and colleagues (2013) note that while the reconstructions based on three model outputs agree well on decadal to multidecadal time periods, they show different sensitivities at centennial resolution (but not the sign). The SAM index (Thompson and Wallace, 2000; Thompson and Solomon, 2002a) was developed during the late 20th Century, at a time when SAM was characterised by a strong positive trend. The SAM$_A$ reconstruction showed that the modern SAM is now at its most positive state of the past millennium (Abram et al., 2014). As a consequence, the reconstructed SAM$_A$ index is mainly negative. To investigate the influence of positive and negative anomalies of the SAM$_A$ relative to its average state over the past 1 ka, we plot the SAM$_A$ reconstruction with an above (light purple) / below (purple) value of its long term average of -1.3 (instead of '0'). The traditional positive SAM$_A$ values (above 0, dark purple) are also shown for reference. Assessing the relationship between RICE, Siple Dome, WDC and TALDICE, we identify three major time periods of change.

6.1   Long-term baseline 660 BCE to 1367 CE

We find that for over 2 ka – from 660 ± 44 years BCE to 1367 ± 12 CE years, the eastern Ross Sea (RICE and Siple Dome) shows an enduring antiphase relationship with West Antarctica (WDC), while coastal East Antarctica in the western Ross Sea (TALDICE) remains neutral (Figure 6). Moreover, with some minor exceptions, isotope and snow accumulation records at RICE, WDC, and TALDICE, respectively, are positively correlated.

6.2   Negative SAM$_A$ - 1368 CE to 1683 CE

The SAM$_A$ reconstruction suggests, that over the past millennium, the SAM was at its most negative (Abram et al., 2014) from 1368 ± 12 years CE to 1683 ± 8 CE years. As noted by Abram et al. (2014), the SAM$_A$ and Niño 3.4 reconstructions (Emile-Geay et al., 2013) are anti-phased on multi-decadal to centennial time scales with the Niño 3.4 index recording some of the warmest SSTs over the past 850 years during this period of negative SAM$_A$.

During the negative SAM$_A$, RICE shows a distinct and sudden increase in isotope temperature, while TALDICE records its coldest conditions over the past 2.7ka, consistent with a negative SAM-forced dipole change in meridional heat flux and surface wind anomalies in the Ross Sea (Marshall and Thompson, 2016). Previously published shorter records from the western Ross Sea from Victoria Lower Glacier in the McMurdo Dry Valleys (Bertler et al., 2011) and Mt Erebus Saddle (Rhodes et al., 2012) also suggest colder conditions in the western Ross Sea during this period, with more extensive sea ice and stronger katabatic flow. We observe that WDC and TALDICE show below average snow accumulation values, while RICE snow accumulation changes from a long-term positive trend to neutral. Such trends are consistent with the reported increased SIE in the western Ross Sea (colder SAT, lower snow accumulation, at TALDICE; and cooler conditions with more extensive sea ice and stronger katabatic winds at Victoria Lower Glacier and Mt Erebus) and Bellingshausen Sea (less snow accumulation, colder SAT at WDC). In contrast, RICE records warmer temperatures along with less and more variable snow accumulation, displaying a distinct Ross Sea Dipole. We suggest that the distinct antiphase relationship is caused by the SAM forcing of equatorward (poleward) heat flux anomalies in the western (eastern) Ross Sea. Coinciding with the sudden increase in RICE

δD in 1492 CE is the decoupling of local temperature from snow accumulation, evident from the diversion of the RICE snow accumulation and δD trends. The reduction in snow accumulation might be linked to a negative SAM-induced weakening of the ASL, leading to the development of fewer blocking events. Alternatively, the abrupt change to warmer temperatures at RICE might also point towards the development of the Roosevelt Island polynya. In recent decades, a Roosevelt Island polynya

5 is observed and merges at times with the much larger Ross Sea polynya (Morales Maqueda et al., 2004). In contrast to the Ross Sea Polynya (Sinclair et al., 2010), a local polynya could provide a potent source for isotopically enriched vapour to precipitation at RICE, perhaps exaggerating the actual warming of the area as interpreted from water stable isotope data. We expect the influence of a Roosevelt Island polynya to have a reduced effect on the more distant Siple Dome, which is consistent with our observations.

6.3   Onset of the positive SAM - 1684 CE to 2012 CE

At 1684 CE $\pm$ 7 years, the SAM_A increases and remains above its long-term average until modern times while the Niño 3.4 index suggests a change to the prevalence of strong La Niña-like conditions. RICE δD suggest the continuation of warm conditions, while snow accumulation drops below the long-term average, with the RICE snow accumulation trend now in-

15 phase with WDC (Figure 6). In contrast, TALDICE records above average snow accumulation rates, which are out of phase with RICE and WDC. Such an alignment is consistent with a positive SAM-forced dipole in meridional heat flux and surface winds (Marshall and Thompson, 2016) between the western Ross Sea (TALDICE) contrasting the eastern Ross Sea (RICE, Siple Dome) and western West Antarctica (WDC). The change to above-average SAM_A (or even positive SAM) values does not coincide with notable changes in any of the isotope records of RICE, Siple Dome or WDC, but concurs with a modest

20 warming of the TALDICE isotope record. However, it marks the onset of the diversion of WDC water isotope and borehole temperature reconstructions. Coincident positive SAM (purple SAM_A values in Figure 6c) and La Niña events have been linked in recent decades to increases in SIE in the western Ross Sea and decreases in the Bellingshausen Sea (Stammerjohn et al., 2008). This is consistent with the notable reduction in snow accumulation at RICE and the trend towards warmer conditions and increased marine air mass intrusions at WDC but is inconsistent with the reduction in snow precipitation at WDC and the

25 trend to warmer conditions at RICE. We interpret the continuation of warm RICE isotope temperatures to reflect the persistence of the Roosevelt Island polynya.

6.4   Dipole pattern on decadal to centennial time scales

To investigate the drivers of decadal to centennial variability, we compare the linearly detrended time series of RICE water stable isotope records with those from (i) Siple Dome and WDC (West Antarctica, Figure 8a) and (ii) TALDICE (East

30 Antarctica, western Ross Sea, Figure 8b). The analysis suggests that until ~200 CE, RICE and Siple Dome (eastern Ross Sea) are in phase with TALDICE variability and thus the East Antarctic climate of the western Ross Sea. From about 400 - 1900 CE, RICE and Siple Dome variability are in-phase with West Antarctic climate variability (WDC). During the negative phase of the SAM_A (Figure 8), the anti-correlation between RICE and TALDICE is particularly strong. Comparable periods of a strong anti-phase relationship occur during 800 - 1200 CE and 300 - 600 CE (grey boxes), perhaps indicative of earlier periods

35 of a strong SAM forcing, albeit a strongly positive SAM with warmer conditions at TALDICE and cooler conditions at RICE. The most recent decades experienced a strong positive SAM influence on the region, which also shows a distinct anti-correlation between RICE and TALDICE and is consistent with this hypothesis.

To assess the correlation of cyclicities apparent in the RICE, Siple Dome, WDC and TALDICE isotope records, wavelet coherence spectrum analyses were conducted (Figure 9) on the time series shown in Figure 8. The analysis of RICE and Siple

40 Dome (Figure 9a) suggests that the two records positively correlate at a broad spectrum of frequencies with cyclicities between 200 – 500 years. The correlation is weakest during 660-100 BCE. A strong anti-phased coherence is also observed for the 30-

70 year periodicity from 0-1000 CE. The high coherency suggests that RICE and Siple Dome respond to similar forcings. The coherence analysis between RICE and WDC shows an enduring in-phase correlations from ~1000 CE to today for the bandwidth of 200 - 700 years. An anti-phase coherence is found from 0 - 500 CE. The coherence analysis between RICE and TALDICE identifies strong relationships predominantly for the early part of the records, from 660 BCE to ~500 CE and a

5   weak coherence from about 1100-1400 CE, when RICE leads by ~75-100 years. The analysis suggests that for the past 2.7 ka the eastern Ross Sea (RICE, Siple Dome) and western West Antarctica (WDC) are climatologically closely linked in their response to forcings on decadal to centennial time scales. The relationship between the western (TALDICE) and eastern (RICE, Siple Dome) Ross Sea experienced a marked change, with a strongly coupled relationship until ~500 CE, which also coincides with opposing climate variability that we interpret to represent a strengthened response to positive and negative SAM forcing

10   of the region.

7   Concluding Remarks

The recent change to a strongly negative SAM (Marshall Index -3.12) in November 2016 coincided with a significant reduction of Antarctic SIE, including the Ross Sea, during the 2016/17 summer (Turner et al., 2017). Longer observations are necessary

15   to assess whether this recent trend continues and indeed forces the reduced SIE, but it fuels questions on the potential acceleration of future environmental change in the Antarctic / Southern Ocean region. To improve projections for the coming decades, an improved understanding of the interplay of teleconnections and local feedbacks is needed.

The Ross Sea region is a climatologically sensitive region that is exposed to tropical and mid-latitude climate drivers. In recent decades, SAM and PSA2 teleconnections lead to opposing effects in the eastern and western Ross Sea region with respect to

20   meridional heat flux, surface wind fields (Marshall and Thompson, 2016), and sea ice extent (Stammerjohn et al., 2008) exhibiting a Ross Sea Dipole. The ASL deepens during combined positive SAM and La Niña events, and weakens during negative SAM and El Niño events. Such interactions have far reaching implications on the regional atmospheric and ocean circulations and sea ice (Turner et al., 2015, Raphael et al., 2016). Additionally, a negative (positive) IPO leads to cooler (warmer) SSTs in the Ross, Amundsen and Bellingshausen seas and has the potential to strengthen (in phase) or weaken (out

25   of phase) the ENSO teleconnection (Henley et al., 2015). Furthermore, the phasing and strength of ENSO events and SAM have been shown to be dependent (Fogt and Bromwich, 2006).

Our data suggest that these dynamically linked climate patterns led to significant and abrupt changes in the past with implications for regional interpretations of trends, including temperature, mass balance and SIE. For over 2 ka, from 660 BCE to the late 14th Century, climate trends in the eastern Ross Sea (RICE and Siple Dome, trend to warmer temperatures and higher

30   precipitation) are anti-correlated with conditions in the western West Antarctica (WDC, cooling with reduced precipitation), while coastal East Antarctica in the western Ross Sea appeared decoupled (TALDICE, no trend in temperature or precipitation). This regional pattern re-organised during a period with strong negative SAM conditions (SAM_A) accompanied by weak La Niña-like conditions (Niño 3.4 index) when western West Antarctica (WDC borehole and isotope temperature) and western Ross Sea (TALDICE) show cold temperatures during the Little Ice Age, while the eastern Ross Sea (RICE, Siple

35   Dome) show warmer or stable temperatures, respectively. In the late 17th Century, the SAM_A changes to above average values, concurrent with a change to strong La Niña-like conditions. These changes establish a strong Ross Sea Dipole that emerges from long-term trend, with western Ross Sea (TALDICE) experiencing warmer temperatures and increased precipitation, while the eastern Ross Sea (RICE, Siple Dome) exhibit reduced precipitation and warmer temperatures. We interpret this pattern to reflect an increase in SIE in the western Ross Sea with perhaps the establishment of the modern Roosevelt Island polynya as

40   a local moisture source for RICE. At the same time, western West Antarctica is showing a warming (WDC borehole temperature) along with an increase in marine air mass intrusions (WDC isotopes) and a reduction in snow accumulation

(WDC). However, when longer-term trends are removed from the correlations, we find earlier periods of a strong Ross Sea dipole which we interpret to reflect previous time periods dominated by strongly positive SAM conditions from the 3rd - 6th Century and 9-12th Century. Our observations are consistent with the reconstruction of the strongly negative SAM from the 14-18th Century and the positive SAM from the 19th Century to today. The continued improvements of array reconstructions

5   (Stenni et al., 2017; Thomas et al., 2017) are an exciting development to further our knowledge of the drivers and effects of past change and their implications for future projections.

Acknowledgments

Funding for this project was provided by the New Zealand Ministry of Business, Innovation, and Employment Grants through
10 Victoria University of Wellington (RDF-VUW-1103, 15-VUW-131) and GNS Science (540GCT32, 540GCT12), and Antarctica New Zealand (K049), the US National Science Foundation (US NSF ANT-0944021, ANT-0944307, ANT-1443472), British Antarctic Survey Funding (BAS PSPE), the Center of Ice and Climate at the Niels Bohr Institute through the Carlsberg Foundation's "North-South Climate Connection" project grant, and the Major State Basic Research Development Program of China (Grant No. 2013CBA01804). We would like to thank Beaudette Ross for conducting gas isotope
15 measurements at the Scripps Institution of Oceanography, University of California, San Diego. Furthermore, we would like to thank Stephen Mawdesley, Grant Kellett, Ryan Davidson, Ed Hutchinson, Bruce Crothers and John Futter of the Mechanical and Electronic Workshops of GNS Science for technical support for the international RICE core progressing campaigns. We are grateful to Diane Bradshaw and Bevan Hunter for their assistance in naming the New Zealand ice core drill. This work is a contribution to the Roosevelt Island Climate Evolution (RICE) Program, funded by national contributions from New Zealand,
20 Australia, Denmark, Germany, Italy, the People's Republic of China, Sweden, UK, and USA. The main logistics support was provided by Antarctica New Zealand (K049) and the US Antarctic Program.

References

25 Abraham, J. P., Baringer, M., Bindoff, N. L., Boyer, T., Cheng, L. J., Church, J. A., Conroy, J. L., Domingues, C. M., Fasullo, J. T., Gilson, J., Goni, G., Good, S. A., Gorman, J. M., Gouretski, V., Ishii, M., Johnson, G. C., Kizu, S., Lyman, J. M., Macdonald, A. M., Minkowycz, W. J., Moffitt, S. E., Palmer, M. D., Piola, A. R., Reseghetti, F., Schuckmann, K., Trenberth, K. E., Velicogna, I., and Willis, J. K.: A review of global ocean temperature observations: Implications for ocean heat content estimates and climate change, Reviews of Geophysics, 51, 450-483, 10.1002/rog.20022, 2013.
30
Abram, N. J., Mulvaney, R., Vimeux, F., Phipps, S. J., Turner, J., and England, M. H.: Evolution of the Southern Annular Mode during the past millennium, Nature Climate Change, 4, 564-569, 2014.

Anderson, R. F., Ali, S., Bradtmiller, L. I., Nielsen, S. H. H., Fleisher, M. Q., Anderson, B. E., and Burckle, L. H.: Wind-
35 Driven Upwelling in the Southern Ocean and the Deglacial Rise in Atmospheric CO2, Science, 323, 1443-1448, 10.1126/science.1167441, 2009.

Arblaster, J., Meehl, G., and Karoly, D.: Future climate change in the Southern Hemisphere: Competing effects of ozone and greenhouse gases, Geophysical Research Letters, 38, 2011.
40
Bakker, P., Clark, P. U., Golledge, N. R., Schmittner, A., and Weber, M. E.: Centennial-scale Holocene climate variations amplified by Antarctic Ice Sheet discharge, Nature, 541, 72-76, 10.1038/nature20582, 2017.

Bertler, N. A. N., Barrett, P. J., Mayewski, P. A., Fogt, R. L., Kreutz, K. J., and Shulmeister, J.: El Niño suppresses Antarctic
45 warming, Geophysical Research Letters, 31, 2004.

Bertler, N. A. N., Mayewski, P. A., and Carter, L.: Cold conditions in Antarctica during the Little Ice Age — Implications for abrupt climate change mechanisms, Earth and Planetary Science Letters, 308, 41-51, 10.1016/j.epsl.2011.05.021, 2011.

5 Bintanja, R., van Oldenborgh, G. J., Drijfhout, S. S., Wouters, B., and Katsman, C. A.: Important role for ocean warming and increased ice-shelf melt in Antarctic sea-ice expansion, Nature Geosci, 6, 376-379, 10.1038/ngeo1767 http://www.nature.com/ngeo/journal/v6/n5/abs/ngeo1767.html#supplementary-information, 2013.

Böning, C. W., Dispert, A., Visbeck, M., Rintoul, S. R., and Schwarzkopf, F. U.: The response of the Antarctic Circumpolar Current to recent climate change, Geoscience Nature, 1, 864-869, 2008.

Bracegirdle, T. J., Turner, J., Hosking, J. S., and Phillips, T.: Sources of uncertainty in projections of twenty-first century westerly wind changes over the Amundsen Sea, West Antarctica, in CMIP5 climate models, Climate Dynamics, 43, 2093-2104, 2014.

15 Braconnot, P., Harrison, S. P., Kageyama, M., Bartlein, P. J., Masson-Delmotte, V., Abe-Ouchi, A., Otto-Bliesner, B., and Zhao, Y.: Evaluation of climate models using palaeoclimatic data, Nature Clim. Change, 2, 417-424, http://www.nature.com/nclimate/journal/v2/n6/abs/nclimate1456.html#supplementary-information, 2012.

Bromwich, D. H., Nicolas, J. P., and Monaghan, A. J.: An Assessment of Precipitation Changes over Antarctica and the 20 Southern Ocean since 1989 in Contemporary Global Reanalyses, Journal of Climate, 24, 4189-4209, 10.1175/2011jcli4074.1, 2011.

Brook, E. J., White, J. W., Schilla, A. S., Bender, M. L., Barnett, B., Severinghaus, J. P., Taylor, K. C., Alley, R. B., and Steig, E. J.: Timing of millennial-scale climate change at Siple Dome, West Antarctica, during the last glacial period, Quaternary 25 Science Reviews, 24, 1333-1343, 2005.

Buiron, D., Chappellaz, J., Stenni, B., Frezzotti, M., Baumgartner, M., Capron, E., Landais, A., Lemieux-Dudon, B., Masson-Delmotte, V., Montagnat, M., Parrenin, F., and Schilt, A.: TALDICE-1 age scale of the Talos Dome deep ice core, East Antarctica, Clim. Past, 7, 1-16, 10.5194/cp-7-1-2011, 2011.

Conway, H., Hall, B. L., Denton, G. H., Gades, A. M., and Waddington, E. D.: Past and Future Grounding-Line Retreat of the West Antarctic Ice Sheet, Science, 286, 280-283, 10.1126/science.286.5438.280, 1999.

DeConto, R. M., and Pollard, D.: Contribution of Antarctica to past and future sea-level rise, Nature, 531, 591-597, 2016.

35

Dee, D. P., Uppala, S. M., Simmons, A. J., Berrisford, P., Poli, P., Kobayashi, S., Andrae, U., Balmaseda, M. A., Balsamo, G., Bauer, P., Bechtold, P., Beljaars, A. C. M., van de Berg, L., Bidlot, J., Bormann, N., Delsol, C., Dragani, R., Fuentes, M., Geer, A. J., Haimberger, L., Healy, S. B., Hersbach, H., Hólm, E. V., Isaksen, L., Kållberg, P., Köhler, M., Matricardi, M., McNally, A. P., Monge-Sanz, B. M., Morcrette, J. J., Park, B. K., Peubey, C., de Rosnay, P., Tavolato, C., Thépaut, J. N., and 40 Vitart, F.: The ERA-Interim reanalysis: configuration and performance of the data assimilation system, Quarterly Journal of the Royal Meteorological Society, 137, 553-597, 10.1002/qj.828, 2011.

DeVries, T., Holzer, M., and Primeau, F.: Recent increase in oceanic carbon uptake driven by weaker upper-ocean overturning, Nature, 542, 215-218, 10.1038/nature21068 45 http://www.nature.com/nature/journal/v542/n7640/abs/nature21068.html#supplementary-information, 2017.

Ding, Q., Steig, E. J., Battisti, D. S., and Küttel, M.: Winter warming in West Antarctica caused by central tropical Pacific warming, Nature Geoscience, 4, 398-403, 2011.

50 Ding, Q., and Steig, E. J.: Temperature change on the Antarctic Peninsula linked to the tropical Pacific, Journal of Climate, 26, 7570-7585, 2013.

Downes, S. M., Bindoff, N. L., and Rintoul, S. R.: Changes in the Subduction of Southern Ocean Water Masses at the End of the Twenty-First Century in Eight IPCC Models, Journal of Climate, 23, 6526-6541, 10.1175/2010jcli3620.1, 2010.

55

Emanuelsson, B. D., Baisden, W. T., Bertler, N. A. N., Keller, E. D., and Gkinis, V.: High-resolution continuous-flow analysis setup for water isotopic measurement from ice cores using laser spectroscopy, Atmos. Meas. Tech., 8, 2869-2883, 10.5194/amt-8-2869-2015, 2015.

60 Emanuelsson, B. D.: High-Resolution Water Stable Isotope Ice-Core Record: Roosevelt Island, Antarctica, PhD, Antarctic Research Centre, Victoria University, Wellington, 2016.

Emanuelsson, B. D., Bertler, N. A. N., Neff, P., D., Renwick, J. A., Markle, B. R., Baisden, W. T., and Keller, E. D.: The role of the Amundsen-Bellingshausen Sea anticyclonic circulation for marine air mass intrusions into West Antarctica, Climate Dynamics, CLDY-D-16-00858, in review.

5   Emile-Geay, J., Cobb, K. M., Mann, M. E., and Wittenberg, A. T.: Estimating Central Equatorial Pacific SST Variability over the Past Millennium. Part II: Reconstructions and Implications, Journal of Climate, 26, 2329-2352, 10.1175/jcli-d-11-00511.1, 2013.

England, M. H., McGregor, S., Spence, P., Meehl, G. A., Timmermann, A., Cai, W., Gupta, A. S., McPhaden, M. J., Purich, 10   A., and Santoso, A.: Recent intensification of wind-driven circulation in the Pacific and the ongoing warming hiatus, Nature Clim. Change, 4, 222-227, 10.1038/nclimate2106 http://www.nature.com/nclimate/journal/v4/n3/abs/nclimate2106.html#supplementary-information, 2014.

Fegyveresi, J. M., Alley, R., Spencer, M., Fitzpatrick, J., Steig, E., White, J., McConnell, J., and Taylor, K.: Late-Holocene 15   climate evolution at the WAIS Divide site, West Antarctica: bubble number-density estimates, Journal of Glaciology, 57, 629-638, 2011.

Ferreira, D., Marshall, J., Bitz, C. M., Solomon, S., and Plumb, A.: Antarctic Ocean and Sea Ice Response to Ozone Depletion: A Two-Time-Scale Problem, Journal of Climate, 28, 1206-1226, 10.1175/jcli-d-14-00313.1, 2015.
20
Fogt, R. L., and Bromwich, D. H.: Decadal Variability of the ENSO Teleconnection to the High-Latitude South Pacific Governed by Coupling with the Southern Annular Mode, Journal of Climate, 19, 979-997, 10.1175/jcli3671.1, 2006.

Fretwell, P., Pritchard, H. D., Vaughan, D. G., Bamber, J. L., Barrand, N. E., Bell, R., Bianchi, C., Bingham, R. G., 25   Blankenship, D. D., Casassa, G., Catania, G., Callens, D., Conway, H., Cook, A. J., Corr, H. F. J., Damaske, D., Damm, V., Ferraccioli, F., Forsberg, R., Fujita, S., Gim, Y., Gogineni, P., Griggs, J. A., Hindmarsh, R. C. A., Holmlund, P., Holt, J. W., Jacobel, R. W., Jenkins, A., Jokat, W., Jordan, T., King, E. C., Kohler, J., Krabill, W., Riger-Kusk, M., Langley, K. A., Leitchenkov, G., Leuschen, C., Luyendyk, B. P., Matsuoka, K., Mouginot, J., Nitsche, F. O., Nogi, Y., Nost, O. A., Popov, S. V., Rignot, E., Rippin, D. M., Rivera, A., Roberts, J., Ross, N., Siegert, M. J., Smith, A. M., Steinhage, D., Studinger, M., Sun, 30   B., Tinto, B. K., Welch, B. C., Wilson, D., Young, D. A., Xiangbin, C., and Zirizzotti, A.: Bedmap2: improved ice bed, surface and thickness datasets for Antarctica, The Cryosphere, 7, 375-393, 10.5194/tc-7-375-2013, 2013.

Fudge, T., Markle, B. R., Cuffey, K. M., Buizert, C., Taylor, K. C., Steig, E. J., Waddington, E. D., Conway, H., and Koutnik, M.: Variable relationship between accumulation and temperature in West Antarctica for the past 31,000 years, Geophysical 35   Research Letters, 43, 3795-3803, 2016.

Gille, S. T.: Warming of the Southern Ocean since 1950s, Science, 295, 1275-1277, 2002.

Gillett, N. P., and Fyfe, J. C.: Annular mode changes in the CMIP5 simulations, Geophysical Research Letters, 40, 1189-1193, 40   10.1002/grl.50249, 2013.

Golledge, N. R., Kowalewski, D. E., Naish, T. R., Levy, R. H., Fogwill, C. J., and Gasson, E. G.: The multi-millennial Antarctic commitment to future sea-level rise, Nature, 526, 421, 2015.

45   Greene, C. A., Gwyther, D. E., and Blankenship, D. D.: Antarctic mapping tools for MATLAB, Computers & Geosciences, 104, 151-157, 2017.

Henley, B. J., Gergis, J., Karoly, D. J., Power, S., Kennedy, J., and Folland, C. K.: A Tripole Index for the Interdecadal Pacific Oscillation, Climate Dynamics, 45, 3077-3090, 10.1007/s00382-015-2525-1, 2015.
50
Holland, M. M., Landrum, L., Kostov, Y., and Marshall, J.: Sensitivity of Antarctic sea ice to the Southern Annular Mode in coupled climate models, Climate Dynamics, 1-19, 10.1007/s00382-016-3424-9, 2016.

Holland, P. R., and Kwok, R.: Wind-driven trends in Antarctic sea-ice drift, Nature Geosci, 5, 872-875, 55   http://www.nature.com/ngeo/journal/v5/n12/abs/ngeo1627.html#supplementary-information, 2012.

Jacobs, S. S., Giulivi, C. F., and Mele, P. A.: Freshening of the Ross Sea During the Late 20th Century, Science, 297, 386-389, 10.1126/science.1069574, 2002.

60   Jacobs, S. S., Jenkins, A., Giulivi, C. F., and Dutrieux, P.: Stronger ocean circulation and increased melting under Pine Island Glacier ice shelf, Nature Geoscience, 4, 519-523, 2011.

Jones, J. M., Gille, S. T., Goosse, H., Abram, N. J., Canziani, P. O., Charman, D. J., Clem, K. R., Crosta, X., de Lavergne, C., and Eisenman, I.: Assessing recent trends in high-latitude Southern Hemisphere surface climate, Nature Climate Change, 6, 917-926, 2016.

5   Joughin, I., and Alley, R. B.: Stability of the West Antarctic ice sheet in a warming world, Nature Geoscience, 4, 506-513, 2011.

Joughin, I., Smith, B. E., and Medley, B.: Marine Ice Sheet Collapse Potentially Under Way for the Thwaites Glacier Basin, West Antarctica, Science, 344, 735-738, 2014.

Kay, S. M.: Modern spectral estimation, Pearson Education India, 1988.

Keller, E. D., Baisden, W. T., Bertler, N. A. N., Emanuelsson, B. D., Phillips, A., and and the RICE team: Calculating uncertainty for the high-resolution RICE ice core continuous flow analysis water isotope record, Atmos. Meas. Tech., in
15   preparation.

Kingslake, J., Hindmarsh, R. C. A., Aðalgeirsdóttir, G., Conway, H., Corr, H. F. J., Gillet-Chaulet, F., Martín, C., King, E. C., Mulvaney, R., and Pritchard, H. D.: Full-depth englacial vertical ice sheet velocities measured using phase-sensitive radar, Journal of Geophysical Research: Earth Surface, 119, 2604-2618, 10.1002/2014jf003275, 2014.

Kohyama, T., and Hartmann, D. L.: Antarctic Sea Ice Response to Weather and Climate Modes of Variability, Journal of Climate, 29, 721-741, 10.1175/jcli-d-15-0301.1, 2015.

Kosaka, Y., and Xie, S.-P.: Recent global-warming hiatus tied to equatorial Pacific surface cooling, Nature, 501, 403-407,
25   10.1038/nature12534, 2013.

Kusahara, K., and Hasumi, H.: Modeling Antarctic ice shelf responses to future climate changes and impacts on the ocean, Journal of Geophysical Research: Oceans, 118, 2454-2475, 10.1002/jgrc.20166, 2013.

30   Küttel, M., Steig, E. J., Ding, Q., Monaghan, A. J., and Battisti, D. S.: Seasonal climate information preserved in West Antarctic ice core water isotopes: Relationships to temperature, large-scale circulation, and sea ice, Climate Dynamics, 39, 1841-1857, 2012.

Landschützer, P., Gruber, N., Haumann, F. A., Rödenbeck, C., Bakker, D. C. E., van Heuven, S., Hoppema, M., Metzl, N.,
35   Sweeney, C., Takahashi, T., Tilbrook, B., and Wanninkhof, R.: The reinvigoration of the Southern Ocean carbon sink, Science, 349, 1221-1224, 10.1126/science.aab2620, 2015.

Lliboutry, L. A.: A critical review of analytical approximate solutions for steady state velocities and temperature in cold ice sheets, Zeitschrift fuer Gletscherkunde, Glazialgeologie, 15, 135-148, 1979.

40

Mandeno, D., Pyne, A. R., Bertler, N. A. N., and Neff, P.: Ice coring at Roosevelt Island: Drill design, performance and refrigeration solutions at a low altitude 'warm coastal' Antarctic location., 7th International Workshop on Ice Core Drilling Technology, Pyle Centre, University of Wisconsin, Madison, USA, 2013.

45   Mantua, N. J., and Hare, S. R.: The Pacific Decadal Oscillation, Journal of Oceanography, 58, 35-44, 10.1023/a:1015820616384, 2002.

Marshall, G. J., Orr, A., and Turner, J.: A Predominant Reversal in the Relationship between the SAM and East Antarctic Temperatures during the Twenty-First Century, Journal of Climate, 26, 5196-5204, 10.1175/jcli-d-12-00671.1, 2013.
50

Marshall, G. J., and Thompson, D. W. J.: The signatures of large-scale patterns of atmospheric variability in Antarctic surface temperatures, Journal of Geophysical Research: Atmospheres, 121, 3276-3289, 10.1002/2015jd024665, 2016.

Marshall, J., and Speer, K.: Closure of the meridional overturning circulation through Southern Ocean upwelling, Nature
55   Geosci, 5, 171-180, 2012.

Masson-Delmotte, V., Hou, S., Ekaykin, A., Jouzel, J., Aristarain, A., Bernardo, R., Bromwich, D., Cattani, O., Delmotte, M., and Falourd, S.: A review of Antarctic surface snow isotopic composition: observations, atmospheric circulation, and isotopic modeling*, Journal of Climate, 21, 3359-3387, 2008.
60

Meehl, G. A., Arblaster, J. M., Fasullo, J. T., Hu, A., and Trenberth, K. E.: Model-based evidence of deep-ocean heat uptake during surface-temperature hiatus periods, Nature Clim. Change, 1, 360-364, http://www.nature.com/nclimate/journal/v1/n7/abs/nclimate1229.html#supplementary-information, 2011.

Meehl, G. A., Arblaster, J. M., Bitz, C. M., Chung, C. T., and Teng, H.: Antarctic sea-ice expansion between 2000 and 2014 driven by tropical Pacific decadal climate variability, Nature Geoscience, 9, 590-595, 2016.

Mo, K. C.: Relationships between Low-Frequency Variability in the Southern Hemisphere and Sea Surface Temperature Anomalies, Journal of Climate, 13, 3599-3610, 10.1175/1520-0442(2000)013<3599:rblfvi>2.0.co;2, 2000.

Morales Maqueda, M. A., Willmott, A. J., and Biggs, N. R. T.: Polynya Dynamics: a Review of Observations and Modeling, Reviews of Geophysics, 42, RG1004, 10.1029/2002rg000116, 2004.

Nicolas, J. P., and Bromwich, D. H.: New Reconstruction of Antarctic Near-Surface Temperatures: Multidecadal Trends and Reliability of Global Reanalyses, Journal of Climate, 27, 8070-8093, 10.1175/jcli-d-13-00733.1, 2014.

Noone, D., and Simmonds, I.: Sea ice control of water isotope transport to Antarctica and implications for ice core interpretation, Journal of Geophysical Research, 109, D07105, 2004.

Orsi, A. J., Cornuelle, B. D., and Severinghaus, J. P.: Little Ice Age cold interval in West Antarctica: evidence from borehole temperature at the West Antarctic Ice Sheet (WAIS) divide, Geophysical Research Letters, 39, 2012.

Pages 2k Consortium: Continental-scale temperature variability during the past two millennia, Nature Geosci, 6, 339-346, 10.1038/ngeo1797
http://www.nature.com/ngeo/journal/v6/n5/abs/ngeo1797.html#supplementary-information, 2013.

Paolo, F. S., Fricker, H. A., and Padman, L.: Volume loss from Antarctic ice shelves is accelerating, Science, 348, 327-331, 10.1126/science.aaa0940, 2015.

Pollard, D., DeConto, R. M., and Alley, R. B.: Potential Antarctic Ice Sheet retreat driven by hydrofracturing and ice cliff failure, Earth and Planetary Science Letters, 412, 112-121, http://dx.doi.org/10.1016/j.epsl.2014.12.035, 2015.

Power, S., Casey, T., Folland, C., Colman, A., and Mehta, V.: Inter-decadal modulation of the impact of ENSO on Australia, Climate Dynamics, 15, 319-324, 10.1007/s003820050284, 1999.

Price, S., Conway, H., and Waddington, E.: Evidence for late pleistocene thinning of Siple Dome, West Antarctica, Journal of Geophysical Research: Earth Surface, 112, 2007.

Pyne, R. L., Keller, E. D., Canessa, S., Bertler, N. A. N., Pyne, A. R., Mandeno, D., Vallelonga, P., Semper, S., Kjær, H. A., and Hutchinson, E.: A noval approach to process brittle ice for continuous flow analysis, Environmental Science & Technology, in review.

Rabiner, L. R., Gold, B., and Yuen, C.: Theory and application of digital signal processing, IEEE Transactions on Systems, Man, and Cybernetics, 8, 146-146, 1978.

Raphael, M., Marshall, G., Turner, J., Fogt, R., Schneider, D., Dixon, D., Hosking, J., Jones, J., and Hobbs, W.: The Amundsen Sea low: Variability, change, and impact on Antarctic climate, Bulletin of the American Meteorological Society, 97, 111-121, 2016.

Raphael, M. N.: A zonal wave 3 index for the Southern Hemisphere, Geophysical Research Letters, 31, n/a-n/a, 10.1029/2004GL020365, 2004.

Raymond, C. F.: Deformation in the vicinity of ice divides, Journal of Glaciology, 29, 357-373, 1984.

Rayner, N. A., Parker, D. E., Horton, E. B., Folland, C. K., Alexander, L. V., Rowell, D. P., Kent, E. C., and Kaplan, A.: Global analyses of sea surface temperature, sea ice, and night marine air temperature since the late nineteenth century, Journal of Geophysical Research: Atmospheres, 108, n/a-n/a, 10.1029/2002jd002670, 2003.

Renwick, J. A.: Persistent Positive Anomalies in the Southern Hemisphere Circulation, Monthly Weather Review, 133, 977-988, 10.1175/mwr2900.1, 2005.

Rhodes, R. H., Bertler, N. A. N., Baker, J. A., Steen-Larsen, H. C., Sneed, S. B., Morgenstern, U., and Johnsen, S. J.: Little Ice Age climate and oceanic conditions of the Ross Sea, Antarctica from a coastal ice core record, Clim. Past Discuss., 8, 215-262, 10.5194/cpd-8-215-2012, 2012.

Rignot, E., Mouginot, J., and Scheuchl, B.: Ice Flow of the Antarctic Ice Sheet, Science, 333, 1427-1430, 10.1126/science.1208336, 2011.

Rignot, E., Mouginot, J., Morlighem, M., Seroussi, H., and Scheuchl, B.: Widespread, rapid grounding line retreat of Pine Island, Thwaites, Smith, and Kohler glaciers, West Antarctica, from 1992 to 2011, Geophysical Research Letters, 2014.

Rintoul, S. R.: Rapid freshening of Antarctic Bottom Water formed in the Indian and Pacific oceans, Geophysical Research Letters, 34, L06606, 10.1029/2006gl028550, 2007.

Russell, J. L., Dixon, K. W., Gnanadesikan, A., Stouffer, R. J., and Toggweiler, J.: The Southern Hemisphere westerlies in a warming world: Propping open the door to the deep ocean, Journal of Climate, 19, 6382-6390, 2006.

Scambos, T., Haran, T., Fahnestock, M., Painter, T., and Bohlander, J.: MODIS-based Mosaic of Antarctica (MOA) data sets: Continent-wide surface morphology and snow grain size, Remote Sensing of Environment, 111, 242-257, 2007.

Schneider, D. P., Steig, E. J., and Van Ommen, T.: High-resolution ice-core stable-isotopic records from Antarctica: towards interannual climate reconstruction, Annals of Glaciology, 41, 63-70, 2005.

Schneider, D. P., and Steig, E. J.: Ice cores record significant 1940s Antarctic warmth related to tropical climate variability, Proceedings of the National Academy of Sciences, 105, 12154-12158, 10.1073/pnas.0803627105, 2008.

Schneider, D. P., Okumura, Y., and Deser, C.: Observed Antarctic Interannual Climate Variability and Tropical Linkages, Journal of Climate, 25, 4048-4066, 10.1175/jcli-d-11-00273.1, 2012.

Sen Gupta, A., Santoso, A., Taschetto, A. S., Ummenhofer, C. C., Trevena, J., and England, M. H.: Projected Changes to the Southern Hemisphere Ocean and Sea Ice in the IPCC AR4 Climate Models, Journal of Climate, 22, 3047-3078, 10.1175/2008jcli2827.1, 2009.

Sinclair, K. E., Bertler, N. A. N., and Trompetter, W. J.: Synoptic controls on precipitation pathways and snow delivery to high-accumulation ice core sites in the Ross Sea region, Antarctica, Journal of Geophysical Research, 115, D22112, 10.1029/2010jd014383, 2010.

Sinclair, K. E., Bertler, N. A. N., Bowen, M. M., and Arrigo, K. R.: Twentieth century sea-ice trends in the Ross Sea from a high-resolution, coastal ice-core record, Geophysical Research Letters, 2014GL059821, 10.1002/2014GL059821, 2014.

Spence, P., Saenko, O. A., Dufour, C. O., Le Sommer, J., and England, M. H.: Mechanisms Maintaining Southern Ocean Meridional Heat Transport under Projected Wind Forcing, Journal of Physical Oceanography, 42, 1923-1931, 10.1175/jpo-d-12-03.1, 2012.

Stammerjohn, S., Massom, R., Rind, D., and Martinson, D.: Regions of rapid sea ice change: An inter-hemispheric seasonal comparison, Geophysical Research Letters, 39, L06501, 10.1029/2012gl050874, 2012.

Stammerjohn, S. E., Martinson, D. G., Smith, R. C., Yuan, X., and Rind, D.: Trends in Antarctic annual sea ice retreat and advance and their relation to El Niño–Southern Oscillation and Southern Annular Mode variability, Journal of Geophysical Research: Oceans, 113, C03S90, 10.1029/2007jc004269, 2008.

Steig, E. J., Schneider, D. P., Rutherford, S. D., Mann, M. E., Comiso, J. C., and Shindell, D. T.: Warming of the Antarctic ice-sheet surface since the 1957 International Geophysical Year, Nature, 457, 459-462, http://www.nature.com/nature/journal/v457/n7228/suppinfo/nature07669_S1.html, 2009.

Steig, E. J., Ding, Q., Battisti, D., and Jenkins, A.: Tropical forcing of Circumpolar Deep Water inflow and outlet glacier thinning in the Amundsen Sea Embayment, West Antarctica, Annals of Glaciology, 53, 19-28, 2012.

Steig, E. J., Ding, Q., White, J. W. C., Kuttel, M., Rupper, S. B., Neumann, T. A., Neff, P. D., Gallant, A. J. E., Mayewski, P. A., Taylor, K. C., Hoffmann, G., Dixon, D. A., Schoenemann, S. W., Markle, B. R., Fudge, T. J., Schneider, D. P., Schauer, A. J., Teel, R. P., Vaughn, B. H., Burgener, L., Williams, J., and Korotkikh, E.: Recent climate and ice-sheet changes in West Antarctica compared with the past 2,000 years, Nature Geosci, 6, 372-375, 10.1038/ngeo1778 http://www.nature.com/ngeo/journal/v6/n5/abs/ngeo1778.html#supplementary-information, 2013.

Stenni, B., Proposito, M., Gragnani, R., Flora, O., Jouzel, J., Falourd, S., and Frezzotti, M.: Eight centuries of volcanic signal and climate change at Talos Dome (East Antarctica), Journal of Geophysical Research: Atmospheres, 107, 2002.

Stenni, B., Buiron, D., Frezzotti, M., Albani, S., Barbante, C., Bard, E., Barnola, J., Baroni, M., Baumgartner, M., and Bonazza, M.: Expression of the bipolar see-saw in Antarctic climate records during the last deglaciation, Nature Geoscience, 4, 46-49, 2011.

Stenni, B., Curran, M. A. J., Abram, N. J., Orsi, A., Goursaud, S., Masson-Delmotte, V., Neukom, R., Goosse, H., Divine, D., van Ommen, T., Steig, E. J., Dixon, D. A., Thomas, E. R., Bertler, N. A. N., Isaksson, E., Ekaykin, A., Frezzotti, M., and Werner, M.: Antarctic climate variability at regional and continental scales over the last 2,000 years, Clim. Past Discuss., 2017, 1-35, 10.5194/cp-2017-40, 2017.

Stouffer, R. J., Eyring, V., Meehl, G. A., Bony, S., Senior, C., Stevens, B., and Taylor, K. E.: CMIP5 Scientific Gaps and Recommendations for CMIP6, Bulletin of the American Meteorological Society, 98, 95-105, 10.1175/bams-d-15-00013.1, 2017.

Thomas, E., and Bracegirdle, T.: Improving ice core interpretation using in situ and reanalysis data, Journal of Geophysical Research: Atmospheres, 114, 2009.

Thomas, E., Dennis, P., Bracegirdle, T. J., and Franzke, C.: Ice core evidence for significant 100-year regional warming on the Antarctic Peninsula, Geophysical Research Letters, 36, 2009.

Thomas, E. R., van Wessem, J. M., Roberts, J., Isaksson, E., Schlosser, E., Fudge, T., Vallelonga, P., Medley, B., Lenaerts, J., Bertler, N., van den Broeke, M. R., Dixon, D. A., Frezzotti, M., Stenni, B., Curran, M., and Ekaykin, A. A.: Review of regional Antarctic snow accumulation over the past 1000 years, Clim. Past Discuss., 2017, 1-42, 10.5194/cp-2017-18, 2017.

Thompson, D., and Solomon, S.: Interpretation of recent Southern Hemisphere climate change, Science, 296, 895-899, 2002a.

Thompson, D. W. J., and Wallace, J. M.: Annular Modes in the Extratropical Circulation. Part I: Month-to-Month Variability, Journal of Climate, 13, 1000-1016, 10.1175/1520-0442(2000)013<1000:amitec>2.0.co;2, 2000.

Thompson, D. W. J., and Solomon, S.: Interpretation of recent Southern Hemisphere climate change, Science, 296, 895-899, 2002b.

Thompson, D. W. J., Solomon, S., Kushner, P. J., England, M. H., Grise, K. M., and Karoly, D. J.: Signatures of the Antarctic ozone hole in Southern Hemisphere surface climate change, Nature Geosci, 4, 741-749, 2011.

Toggweiler, J. R., and Russell, J.: Ocean circulation in a warming climate, Nature, 451, 286-288, 2008.

Trenberth, K. E., and Stepaniak, D. P.: Indices of El Niño Evolution, Journal of Climate, 14, 1697-1701, 10.1175/1520-0442(2001)014<1697:lioeno>2.0.co;2, 2001.

Tuohy, A., Bertler, N., Neff, P., Edwards, R., Emanuelsson, D., Beers, T., and Mayewski, P.: Transport and deposition of heavy metals in the Ross Sea Region, Antarctica, Journal of Geophysical Research: Atmospheres, 120, 10,996-911,011, 10.1002/2015jd023293, 2015.

Turner, J., Phillips, T., Hosking, J. S., Marshall, G. J., and Orr, A.: The Amundsen Sea Low, International Journal of Climatology, 33, 1818-1829, 2013.

Turner, J., Phillips, T., Marshall, G. J., Hosking, J. S., Pope, J. O., Bracegirdle, T. J., and Deb, P.: Unprecedented springtime retreat of Antarctic sea ice in 2016, Geophysical Research Letters, n/a-n/a, 10.1002/2017gl073656, 2017.

Vinther, B. M., Buchardt, S. L., Clausen, H. B., Dahl-Jensen, D., Johnsen, S. J., Fisher, D. A., Koerner, R. M., Raynaud, D., Lipenkov, V., Andersen, K. K., Blunier, T., Rasmussen, S. O., Steffensen, J. P., and Svensson, A. M.: Holocene thinning of the Greenland ice sheet, Nature, 461, 385-388, http://www.nature.com/nature/journal/v461/n7262/suppinfo/nature08355_S1.html, 2009.

WAIS Divide Project Members: Onset of deglacial warming in West Antarctica driven by local orbital forcing, Nature, 500, 440-444, 2013.

Wang, S., Huang, J., He, Y., and Guan, Y.: Combined effects of the Pacific Decadal Oscillation and El Niño-Southern Oscillation on Global Land Dry–Wet Changes, Scientific Reports, 4, 6651, 10.1038/srep06651 https://www.nature.com/articles/srep06651#supplementary-information, 2014.

Wang, Y., Ding, M., Wessem, J. M. v., Schlosser, E., Altnau, S., Broeke, M. R. v. d., Lenaerts, J. T. M., Thomas, E. R., Isaksson, E., Wang, J., and Sun, W.: A Comparison of Antarctic Ice Sheet Surface Mass Balance from Atmospheric Climate Models and In Situ Observations, Journal of Climate, 29, 5317-5337, 10.1175/jcli-d-15-0642.1, 2016.

Winstrup, M., Svensson, A. M., Rasmussen, S. O., Winther, O., Steig, E. J., and Axelrod, A. E.: An automated approach for annual layer counting in ice cores, Clim. Past, 8, 1881-1895, 10.5194/cp-8-1881-2012, 2012.

Winstrup, M., Vallelonga, P., Kjær, H. A., Fudge, T. J., Lee, J. E., Riis, M. H., Edwards, R., Bertler, N. A. N., Blunier, T., Brook, E., Buizert, C., Ciobanu, G., Conway, H., Dahl-Jensen, D., Ellis, A., Emanuelsson, D., Kurbatov, A., Mayewski, P., Neff, P. D., Pyne, P. E., Simonsen, M. F., Svensson, A., Tuohy, A., and Waddington, E. D.: A 2700-year timescale and accumulation reconstruction for Roosevelt Island, West Antarctica, Climate of the Past, in preparation.

Wong, A. P. S., Bindoff, N. L., and Church, J. A.: Large-scale freshening of intermediate waters in the Pacific and Indian oceans, Nature, 400, 440-443, 1999.

Yuan, X., and Martinson, D. G.: The Antarctic dipole and its predictability, Geophysical Research Letters, 28, 3609-3612, 10.1029/2001GL012969, 2001.

Table 1: Overview of ice core records used in this manuscript. Locations are present in Figure 1.

Name	Location		Elevation (m)	Drill Depth (m)	Year Recovered	Reference
RICE Deep	S 79.3640	W 161.706	550	8.57-764.60	2011/12 (0-130m) and 2012/13 (130-764.60m)	This paper
RICE 12/13 B	S 79.3621	W 161.700	550	0-19.41	2012/13	This paper
WDC	S 79.47	W 112.09	1,766	3,405	2006-11	Steig et al. 2013, Fudge et al. 2016
Siple Dome	S 81.65	W 148.81	620	1,004	1997-99	WAIS Divide Members, 2013; Brook et al., 2005
TALDICE	S 72.78	E 159.07	2,318	1,620	2005-07	Stenni et al. 2011, Buiron et al. 2011

Table 2: Overview of correlation coefficients for annual means of the common time period 1979-2012 between climate parameters, proxies and indices: the original RICE (δD) and optimised (δD$_o$) data (this paper), the original RICE snow accumulation data (RICE Acc, Winstrup 10 et al., in preparation) and data adjusted to the revised age scale of δD$_o$ – Acc$_o$. ERAi Surface Temperature (ERAi SAT) and Precipitation (ERAi Precip), Dee at el., 2011), Ross/Amundsen Sea Sea Ice Extent (SIE$_J$, Jones et al., 2016), Southern Annular Mode Index (SAM$_A$, Abram et al., 2014), Southern Oscillation Index (SOI, Trenberth and Stepaniak, 2001), Niño 4 Index (Trenberth and Stepaniak, 2001) and Niño 3.4 (Emile-Geay et al., 2013), Inter-decadal Pacific Oscillation Index (IPO, Henley et al.,2015), and the near-surface Antarctic temperature reconstruction (NB2014, Nicolas and Bromwich, 2014). Significance values are adjusted for degree of freedom depending on 15 the length of the time series. Only correlation coefficients exceeding 95% (r≥0.34, n=34) are shown; bold-italic values exceed 99% (r≥0.42, n=34); bold values exceed 99.9% (r≥0.54, n=34). SAM$_A$ and IPO have been adjusted for a lower degree of freedom (df=28) as the reconstructions end in 2007. Nss denotes 'not statistically significant'. Correlation between RICE δD and RICE Acc is r=0.40, p<0.05; RICE δD$_o$ and RICE Acc$_o$ is r=0.45, p<0.01.

R	ERAi SAT	ERAi Precip	SIE$_J$	SAM$_A$	SOI	Niño 4	Niño 3.4	IPO	NB2014
RICE δD/δD$_o$	*0.45/0.75*	*0.13/0.49*	*-0.37/-0.53*	nss/-0.40	nss/nss	nss/nss	nss/nss	nss/nss	nss/nss
RICE Acc/Acc$_o$	**0.60**/0.34	**0.67**/0.34	**-0.56**/*-0.42*	*-0.46*/nss	nss/nss	nss/nss	nss/nss	nss/nss	nss/nss
ERAi SAT	x	**0.66**	-0.38	*-0.49*	nss	nss	nss	Nss	nss
ERAi Precip	**0.66**	x	*-0.67*	*-0.42*	*-0.49*	0.37	0.39	*0.44*	nss
SIE$_J$	-0.38	**-0.67**	x	*0.45*	**0.55**	*-0.48*	*-0.48*	**-0.58**	nss
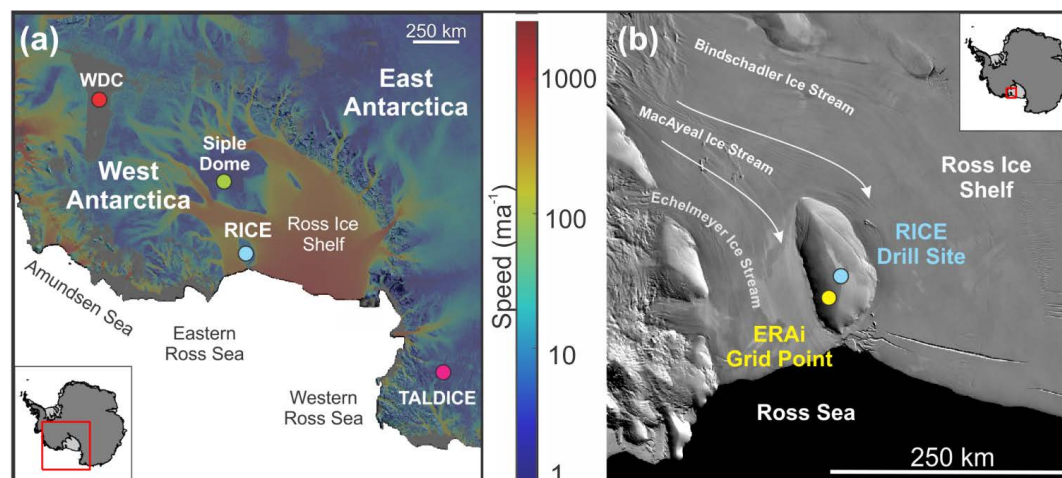
Figures

Figure 1: (a) Overview map of the Ross Sea region and eastern West Antarctica. Antarctic ice velocity derived from ALOS PALSAR, Envisat ASAR, RADARSAT- 2 and ERS-1/2 satellite radar interferometry colour coded on a logarithmic scale (Rignot et al., 2011). (b) Overview map of Roosevelt Island derived from Modis satellite images (Scambos et al., 2007). The maps were created using the Antarctic Mapping Tool (Greene et al., 2017)
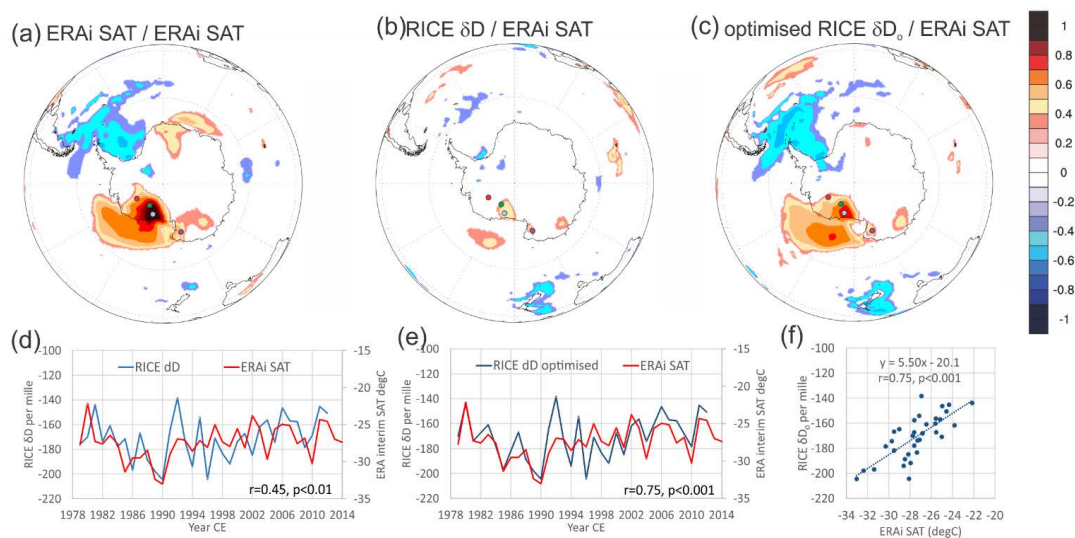
Figure 2: Spatial correlation fields exceeding ≥ 95% significance between a) ERAi annual SAT at the RICE site with ERAi annual SAT in the Antarctic / Southern Ocean region and b) ERAi annual SAT and annually averaged RICE δD data, c) as for b but with 10 **optimised RICE δD data alignment within the dating uncertainty. The correlation has been performed using ClimateReanalyzer.Org, University of Maine, USA, d) time series of ERAi SAT and RICE δD data, e) time series of ERAi SAT and optimised RICE δD data alignment, and f) scatter plot between RICE δD$_o$ and ERAi SAT. The coloured dots indicate the locations of the drill sites – RICE (blue), Siple Dome (green), WDC (red), and TALDICE (pink)**
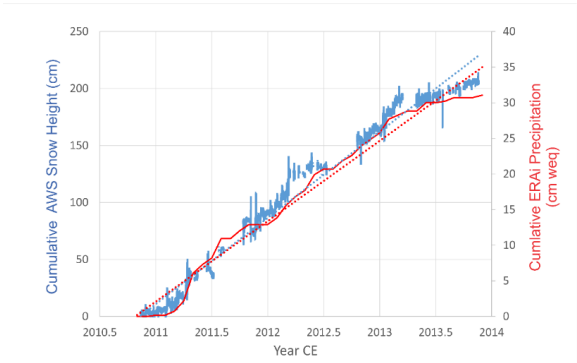
Figure 3: Comparison of snow accumulation data recorded by the RICE AWS (blue) in cumulative snow height in cm and ERAi precipitation values (red) in cm water equivalent cumulative height for the RICE Drill Location. Dotted blue and red lines indicate linear trends for AWS and ERAi data, respectively.
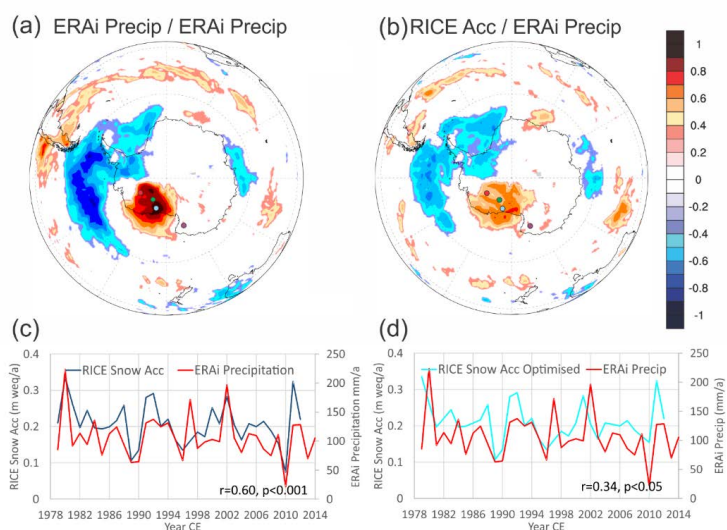
Figure 4: a) Spatial correlation between ERAi annual precipitation at the RICE site with ERAi annual precipitation in the Antarctic / Southern Ocean region and b) spatial correlation between ERAi annual precipitation and annually averaged RICE snow accumulation data. Only fields exceeding ≥ 95% significance are shown. The correlation has been performed using ClimateReanalyzer.Org, University of Maine, USA. Coloured dots indicate locations of WDC (red), Siple Dome (green), RICE (blue) and TALDICE (purple)
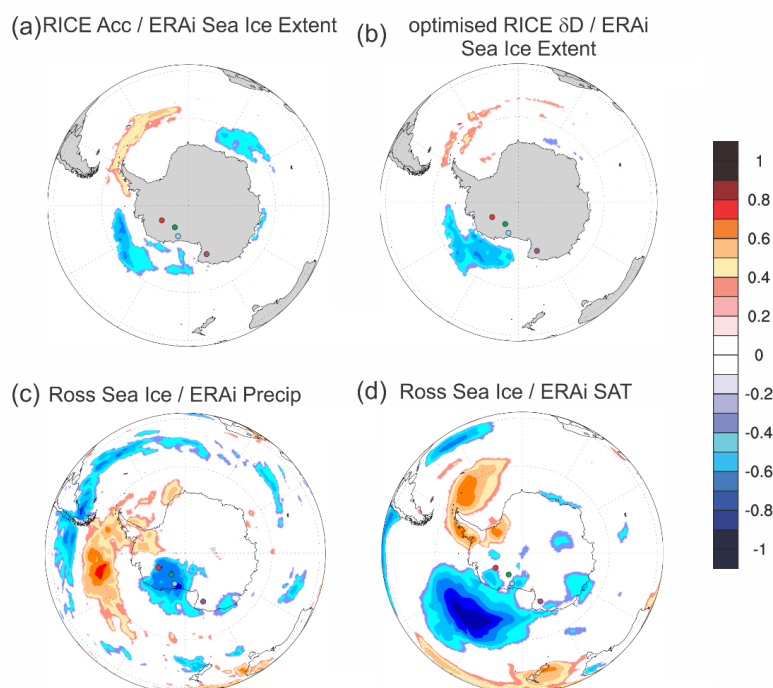
5   **Figure 5: Upper panels: Spatial correlation of ERAi sea ice concentration (SIC) fields with the time series of a) RICE snow accumulation and b) RICE δDo. Lower panels: spatial correlation of the Ross-Amundsen Sea Sea Ice Extent (SIE_J) time series (Jones et al., 2016) with c) ERAi Precipitation and d) ERAi SAT fields. Only fields exceeding ≥ 95% significance are shown. The correlation has been performed using ClimateReanalyzer.Org, University of Maine, USA.**
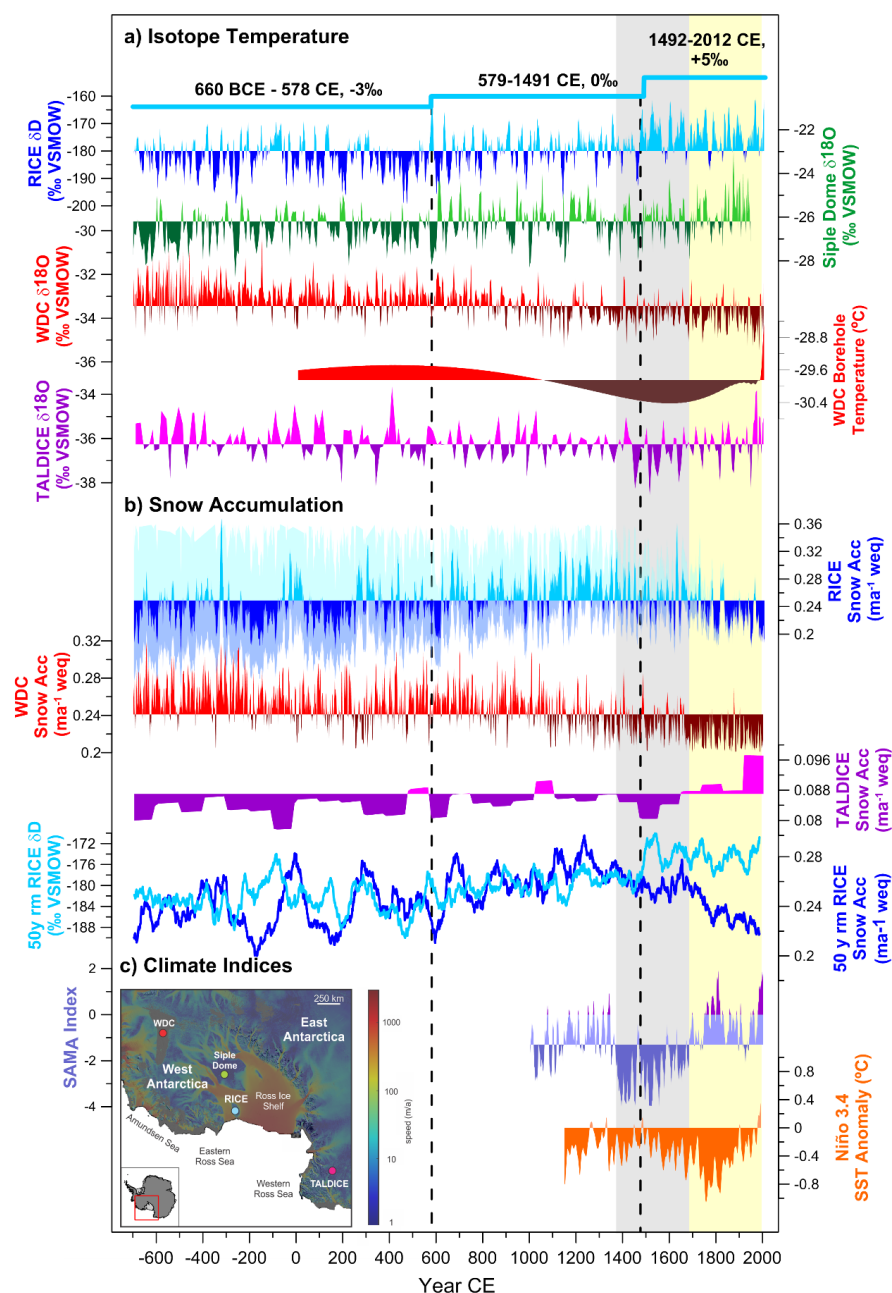
Figure 6: a) Isotope records for the past 2,700 years for RICE, Siple Dome (Brook et al., 2005; WAIS Divide Project Members, 2013), WDC (WAIS Divide Project Members, 2013) and TALDICE (Stenni et al., 2011); **b)** snow accumulation data for RICE (Winstrup et al., in preparation), WDC (Fudge et al., 2016), and TALDICE (Buiron et al., 2011). No snow accumulation data are available for Siple Dome; **c)** Reconstructions of Climate Indices for SAM$_A$ (Abram et al., 2014) and Niño 3.4 based on HadSST2 (Emile-Geay et al., 2013). Colour coding identifies above and below average values. Grey shaded area emphasises period of negative SAMA, yellow shaded area emphasises period of synchronous warming at RICE, Siple Dome, WDC and TALDICE.
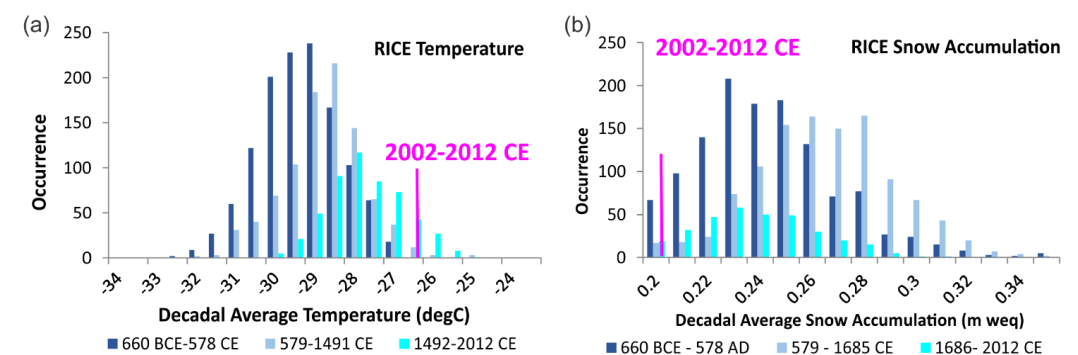
Figure 7: a) Frequency occurrences of decadal temperature variations (10 year moving averages) as reconstructed from the RICE ice core are shown for three periods: 660 BCE to 578 CE – dark blue, 579-1491 CE – light blue, and 1492-2012 CE -cyan. The 10 year average temperature for the most recent decade contained in the record, 2002-2012, -25.78 deg C, is shown in pink. b) Frequency occurrences of decadal RICE snow accumulation variations (10 year moving averages for 660 CE to 578 CE – dark blue, 579-1685 CE – light blue, and 1686-2012 CE - cyan. The 10 year average for the most recent contained in the record, 2002-2012, 0.2m weq is shown in pink.
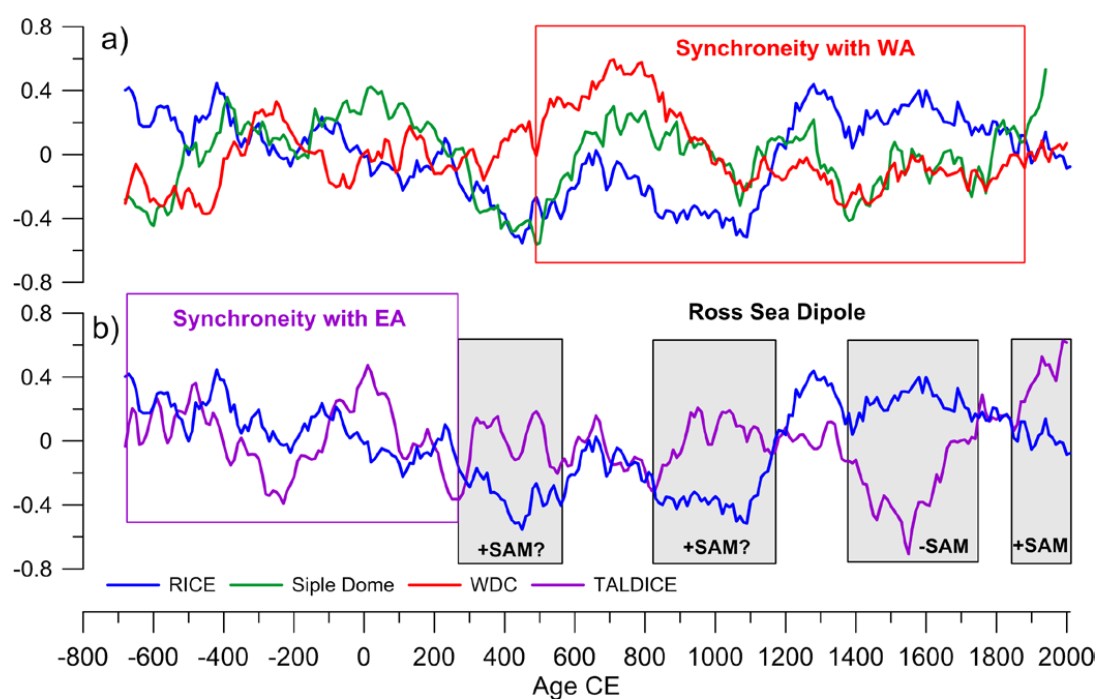
Figure 8: Phasing of multi-decadal and centennial climate variability at RICE, Siple Dome, WDC and TALDICE using detrended, normalised records smoothed with a 200-year moving average. RICE and Siple Dome are compared with a) WDC and b) TALDICE to investigate phase relationships of climate variability in the eastern Ross Sea with West (WDC) and East Antarctica (TALDICE). WA= West Antarctica, EA= East Antarctica. The boxes indicate periods of synchroneity of RICE and Siple Dome records with WA (red box) or EA (purple box). Black boxes indicate time periods where RICE (eastern Ross Sea) shows a strong antiphase relationship (a Ross Sea Dipole) with TALDICE (western Ross Sea).
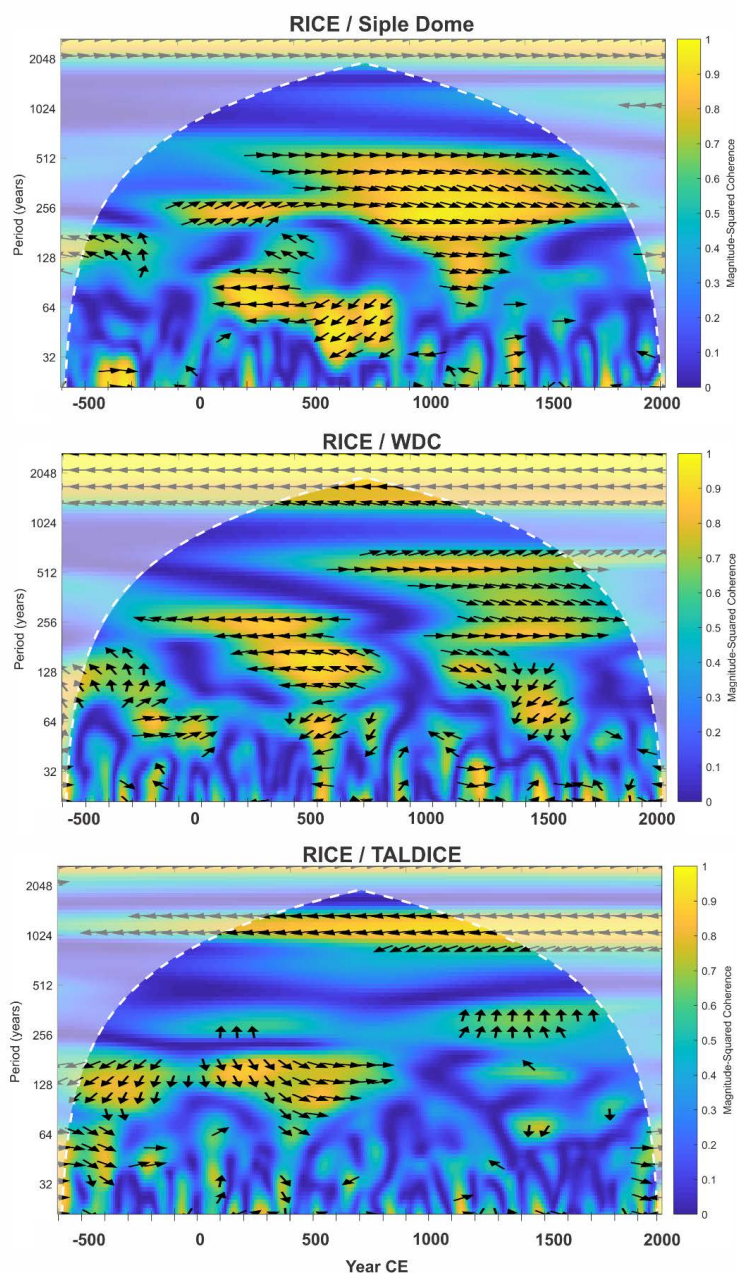
Figure 9: Wavelet coherence and cross spectrum analysis of a) RICE δD and Siple Dome δ¹⁸O, b) RICE δD and WDC δ¹⁸O, c) RICE δD and TALDICE δ¹⁸O. The Analysis was conducted on decadally averaged, detrended data, smoothed with a 200 year moving average. The coherence is computed using the Morlet wavelet and is expressed as magnitude-squared coherence (msc). The phase of the wavelet cross-spectrum is provide for values over 0.6 msc using a Welch's overlapped averaged periodogram method (Rabiner et al., 1978; Kay, 1988). Arrows to the right indicate RICE is leading, arrows the left indicate RICE is lagging. An upright or downward arrow represents ¼ cycle difference.